Analogous carbene-stabilised $[M^{I}\text{-}(\eta^{6}\text{-tol})]^{+}$ cations (M = Fe, Co, Ni): synthetic access and $[carbene{\cdot}M^{I}]^{+}$ transfer

Annika Schulz,[a] and Terrance J. Hadlington*,[a]

[a] Lehrstuhl für anorganische Chemie mit Schwerpunkt neue Materialien, School of Natural Sciences, Technische Universität München, Lichtenberg Strasse 4, 85747 Garching

1. Experimental methods and data

General considerations. All experiments and manipulations were carried out under dry oxygen free argon atmosphere using standard Schlenk techniques or in a MBraun inert atmosphere glovebox containing an atmosphere of high purity argon. THF and diethyl ether were dried by distillation over a sodium/benzophenone mixture and stored over activated 4Å mol sieves. C_6D_6 was dried, degassed and stored over a potassium mirror. All other solvents were dried over activated 4Å mol sieves and degassed prior to use. $[FeCp_2][BAr^F{}_4]$ ($Ar^F{}_4$ = 3,5-$(CF_3)_2$-C_6H_3),[1] IPr·Fe·[η^2-$(vtms)_2$],[2] IPr·Co·[η^2-$(vtms)_2$],[3] and IPr·Ni·[η^2-$(vtms)_2$],[4] were synthesized according to modified known literature procedures. All other reagents were used as received. NMR spectra were recorded on a Bruker AV 400 Spectrometer. The ^1H and $^{13}C\{^1H\}$ NMR spectra were referenced to the residual solvent signals as internal standards. Liquid Injection Field Desorption Ionization Mass Spectrometry (LIFDI-MS) was measured directly from an inert atmosphere glovebox with a Thermo Fisher Scientific Exactive Plus Orbitrap equipped with an ion source from Linden CMS.[5] The compounds were measured as solids under inert conditions in the glovebox. Absorption spectra (UV/vis) were recorded on an Agilent Cary 60 UV/vis spectrophotometer. Elemental analyses (C, H, N) were performed with a combustion analyzer (elementar vario EL, Bruker).

Synthetic details and data

General synthetic procedure for [IPr·M·(η^6-tol)][BAr$^F_4$] complexes. [IPr·M·(η^2-vtms)$_2$] was dissolved in toluene (20 mL), and added to solid [Fc][BAr$^F_4$] (1 eq.) which had been pre-cooled to -80°C. The reaction mixture was stirred at this temperature for 10 min, and subsequently warmed to room temperature and stirred overnight. Over this time, the respective [IPr·M·(η^6-tol)][BAr$^F_4$] complex precipitated/deposited as an oil or oily solid. The reaction mixture was then filtered/decanted, and the solid/oily residue washed with pentane (10 mL), leading to the complete precipitation of the products as a coloured solid residue. These decanting and washing steps also ensure removal of the ferrocene by-product. Subsequently, the remaining residue was redissolved in PhF (3 mL), and recrystallized by layering with pentane (15 mL) at room temperature. After storage for 24 h, crystals suitable for SCXRD were obtained.

[IPr·Fe·(η^6-tol)][BAr$^F_4$], 1. The complex was obtained following the general procedure, using [IPr·Fe·(η^2-(vtms)$_2$] (200 mg, 0.31 mmol). Complex **1** was isolated as a purple solid (280 mg, 0.20 mmol, 65%).

^{1}H NMR (THF-*d*^{8}, 400 MHz, 298 K): -25.70, -18.19, 0.63, 1.93, 7.52, 7.73, 15.19, 18.23, 19.24, 24.37.

Magnetic moment (SQUID; crystalline solid, 298 K): 4.13 μ_B.

MS/LIFDI-HRMS found (calcd.) m/z: 536.2776 (536.2848) [M-BAr$^F_4$]$^+$.

Anal. calcd. for $C_{66}H_{56}BFeF_{24}N_2$: C, 56.63%; H, 4.03%; N, 2.00%; found C, 55.78%; H, 4.09%; N, 2.17%.

[IPr·Co·(η^6-tol)][BAr$^F_4$], 2. The complex was obtained following the general procedure, using [IPr·Co·(η^2-(vtms)$_2$] (200 mg, 0.31 mmol). Complex **2** was isolated as a green solid (330 mg, 0.24 mmol, 76%).

^{1}H NMR (THF-*d*^{8}, 400 MHz, 298 K): -4.38, -0.93, 1.92, 7.56, 7.79, 8.11, 10.22, 11.69.

Magnetic moment (Evans' method; THF-*d*^{8}, 400 MHz, 298 K): 2.85 μ_B. (SQUID; crystalline solid, 298 K): 3.92 μ_B.

MS/LIFDI-HRMS found (calcd.) m/z: 539.2811 (539.2836) for [M-BAr$^F_4$]$^+$.

Anal. calcd. for $C_{66}H_{56}BCoF_{24}N_2$: C, 56.51%; H, 4.02%; N, 2.00%; found C, 55.69%; H, 4.04%; N, 2.04%.

[IPr·Ni·(η^6-tol)][BAr$^F_4$]. 3. The complex was obtained following the general procedure, using [IPr·Ni·(η^2-(vtms)$_2$] (350 mg, 0.54 mmol). Compound **3** was isolated as a yellow solid (510 mg, 0.36 mmol, 67%).

^{1}H NMR (THF-*d*^{8}, 400 MHz, 298 K): -0.12, 2.32, 3.35, 6.49, 7.08-7.22, 7.65, 7.84, 11.86, 18.51.

Magnetic moment (Evans' method; THF-*d*^{8}, 400 MHz, 298 K): 2.09 μ_B. (SQUID; crystalline solid, 298 K): 2.04 μ_B.

MS/LIFDI-HRMS found (calcd.) m/z: 538.2874 (538.2852) [M-BAr$^F_4$]$^+$.

Anal. calcd. for $C_{66}H_{56}BNiF_{24}N_2$: C, 56.52%; H, 4.02%; N, 2.00%; found C, 56,28%; H, 4.05%; N, 2.03%.

[IPr$_2$·Fe][BAr$^F_4$], 4. Complex **1** (150 mg, 0.11 mmol) and IPr (42 mg, 0.11 mmol) were added to a Schlenk flask, the flask precooled to -80 °C, and diethyl ether (20 mL) added. After stirring at this temperature for 10 min, the reaction mixture was allowed to warm to room temperature, whereby the colour changed from purple to red. After 1 h of stirring, the reaction mixture was filtered and concentrated to ~5 mL. Red-orange crystals of **4** suitable for SCXRD were obtained following storage of this solution overnight (125 mg, 0.074 mmol, 69%).

^{1}H NMR (THF-d^8, 400 MHz, 298 K): -25.62, -18.10, 0.72, 7.68, 7.91, 18.32, 19.33, 24.47.

MS/LIFDI-HRMS found (calcd.) m/z: 832.5130 (832.5101) [M-BAr$^F_4$]$^+$.

Magnetic moment (Evans' method; THF-d^8, 400 MHz, 298 K): 2.28 μ_B.

Anal. calcd. for $C_{86}H_{84}BFeF_{24}N_4$: C, 60.90%; H, 4.99%; N, 3.30%; found C, 60.20%; H, 4.90%; N, 3.29%.

[IPr$_2$·Co][BAr$^F_4$], 5. Complex **2** (200 mg, 0.14 mmol) and IPr (55 mg, 0.14 mmol) were added to a Schlenk flask, the flask precooled to -80 °C, and diethyl ether (20 mL) added. After stirring at this temperature for 10 min, the reaction mixture was allowed to warm to room temperature, whereby the colour changed from green to dark yellow. After 30 minutes of stirring, the reaction mixture was filtered and concentrated to ~5 mL. Orange crystals of **5** suitable for SCXRD were obtained following storage of this solution overnight (180 mg, 0.11 mmol, 74%).

^{1}H NMR (THF-d^8, 400 MHz, 298 K): -33.91, -28.94, -0.01, 7.07, 7.30, 8.14, 9.50, 17.37.

MS/LIFDI-HRMS found (calcd.) m/z: 835.5103 (835.5083) for [M-BAr$^F_4$]$^+$.

Anal. calcd. for $C_{86}H_{84}BCoF_{24}N_4$: C, 60.79%; H, 4.98%; N, 3.30%; found C, 59.94%; H, 4.93%; N, 3.48%.

[IPr$_2$·Ni][BAr$^F_4$], 6. Complex **3** (150 mg, 0.11 mmol) and IPr (42 mg, 0.11 mmol) were added to a Schlenk flask, the flask precooled to -80 °C, and diethyl ether (20 mL) added. After stirring at this temperature for 10 min, the reaction mixture was allowed to warm to room temperature, whereby the colour changed from pale yellow to green. After 1 hour of stirring, the reaction mixture was filtered and concentrated to ~5 mL. Colourless crystals of **6** suitable for SCXRD were obtained following storage of this solution overnight (130 mg, 0.077 mmol, 72%).

^{1}H NMR (THF-d^8, 400 MHz, 298 K): -11.72, -8.85, -0.43, 0.06, 5.46, 7.35, 7.57, 8.21, 8.30, 9.57.

MS/LIFDI-HRMS found (calcd.) m/z: 834.5097 (834.5105) [M-BAr$^F_4$]$^+$.

Magnetic moment (Evans' method; THF-d^8, 400 MHz, 298 K): 3.00 μ_B.

Anal. calcd. for $C_{86}H_{84}BNiF_{24}N_4$: C, 60.78%; H, 4.98%; N, 3.30%; found C, 60.29%; H, 5.07%; N, 3.40%.

NMR, MS, UV/vis, and SQUID graphical data

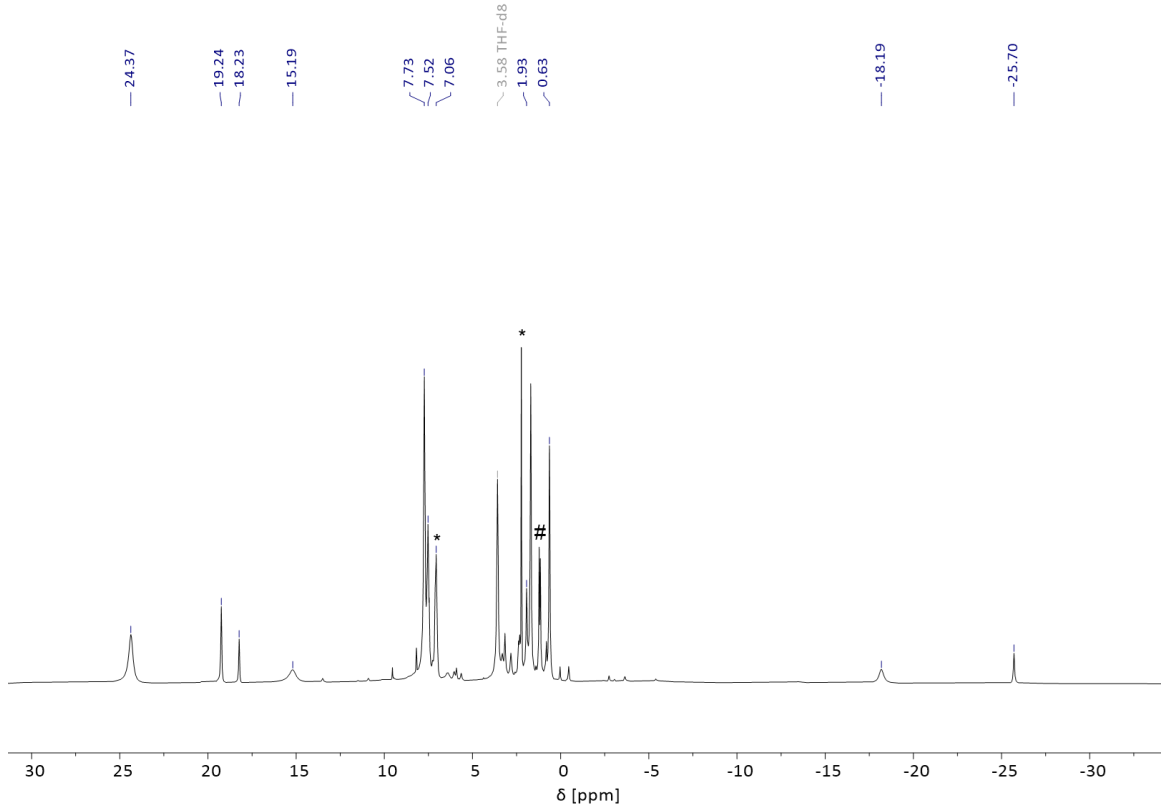

Figure S1. ^{1}H NMR spectrum of **1** as a solution in THF-d^8 at ambient temperature; * indicates small amounts of free ^{Dipp}NHC.

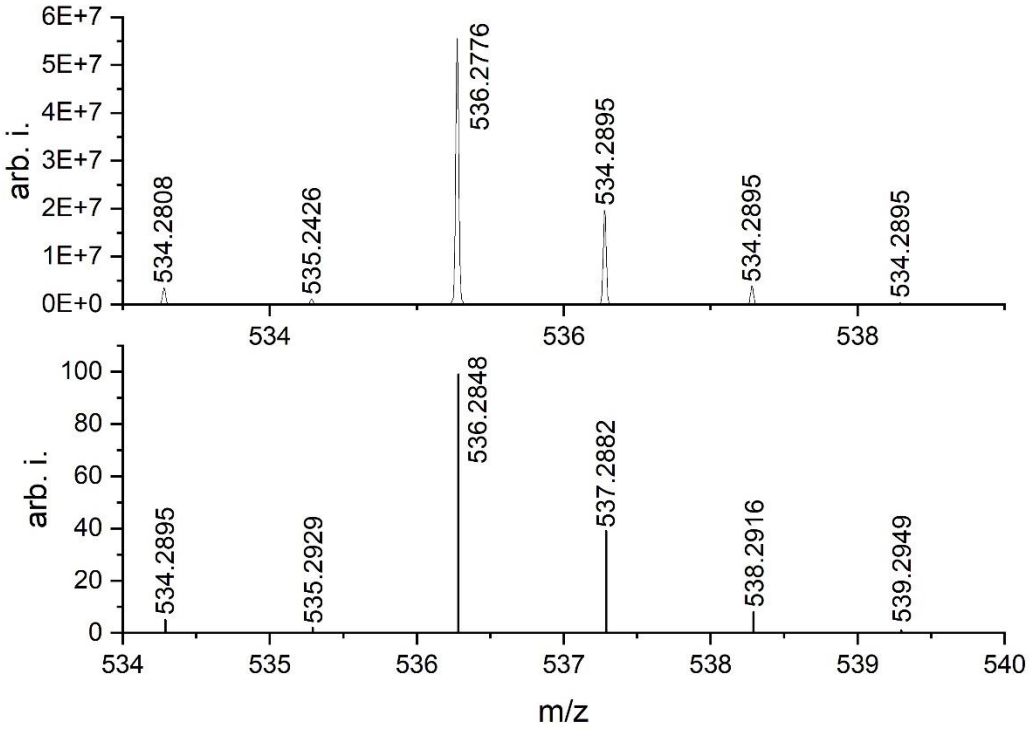

Figure S2. *Top:* Cutout from LIFDI/MS of **1;** *Bottom:* Calculated MS spectrum of [**1**-BAr_4^F]$^+$.

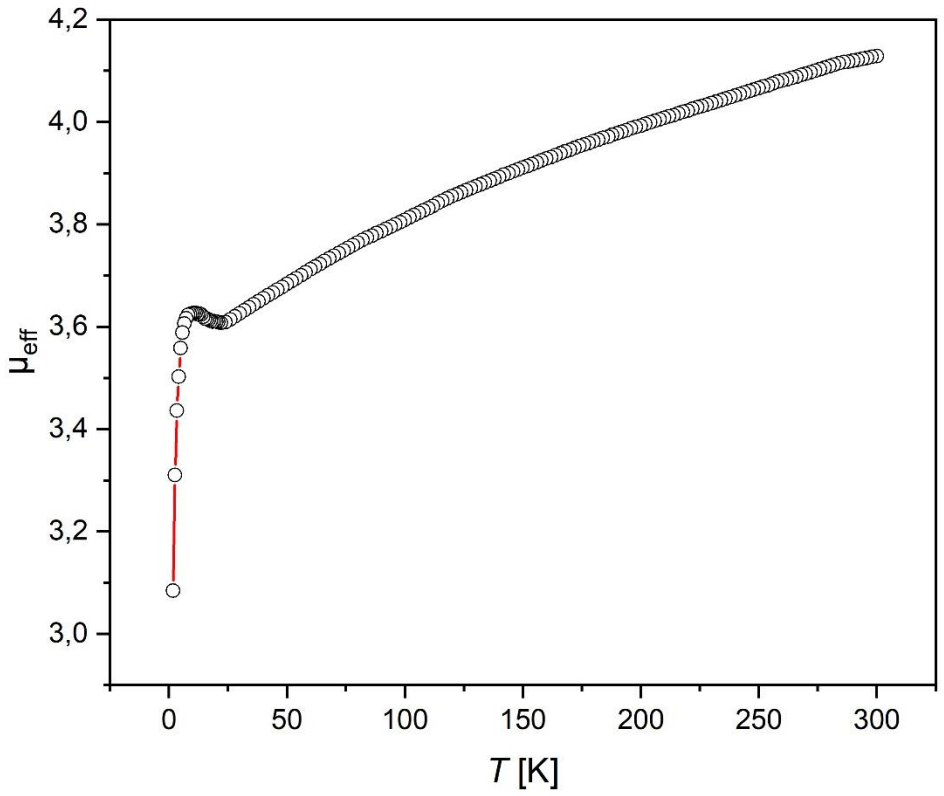

Figure S3. Effective magnetic moment μ_{eff} of a crystalline sample of **1** from 1.8 K to 300 K.

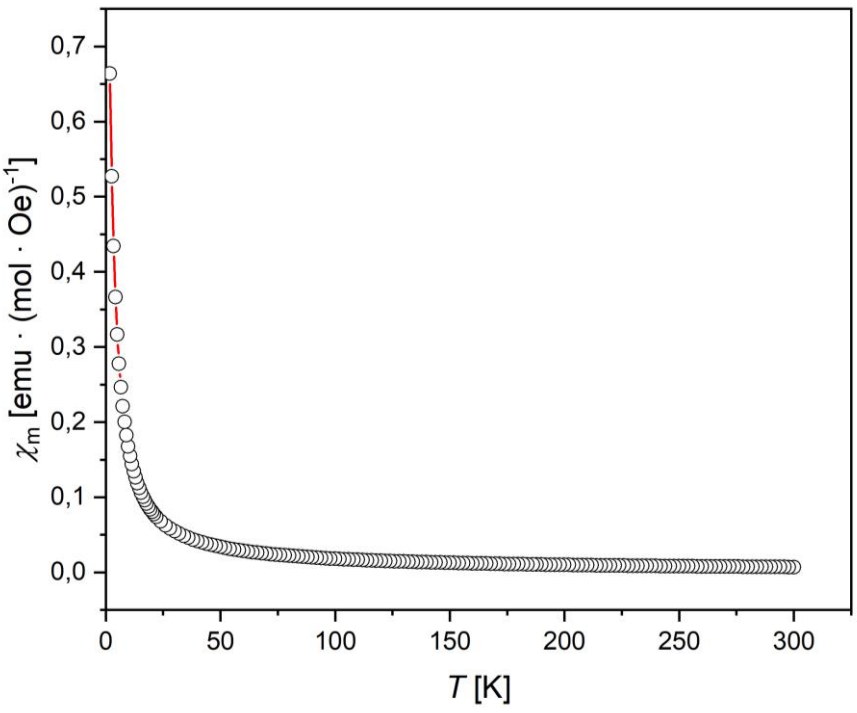

Figure S4. Magnetic susceptibility χ_M of a crystalline sample of **1** from 1.8 K to 300 K.

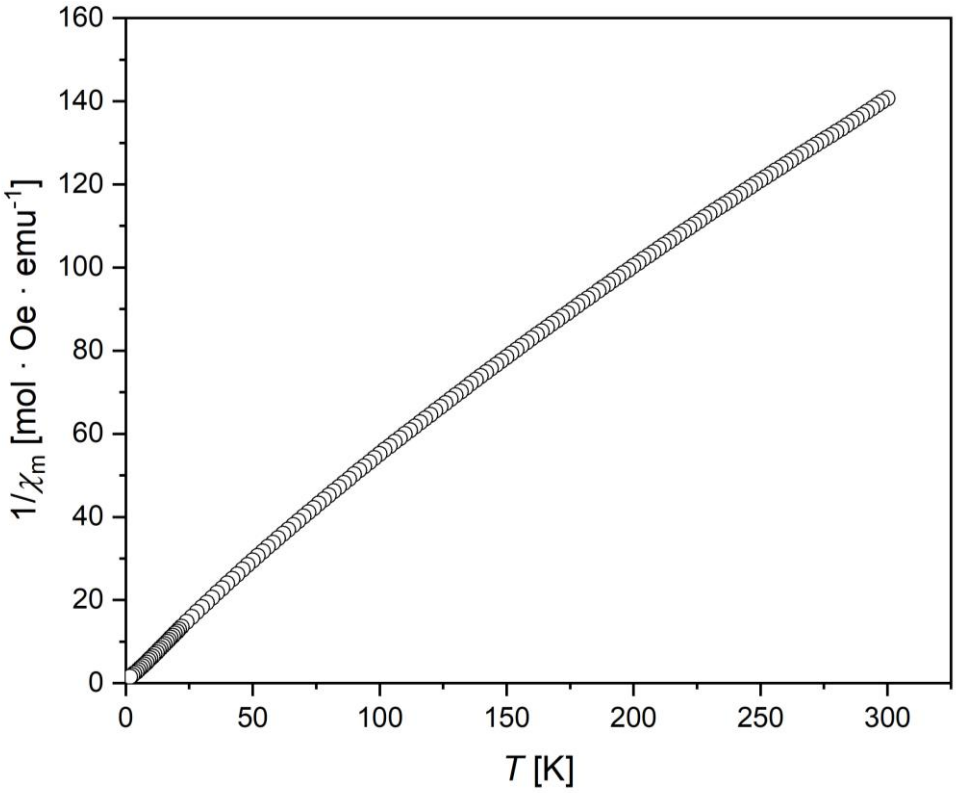

Figure S5. Inverse of the magnetic susceptibility $1/\chi_M$ of a crystalline sample of **1** from 1.8 K to 300 K.

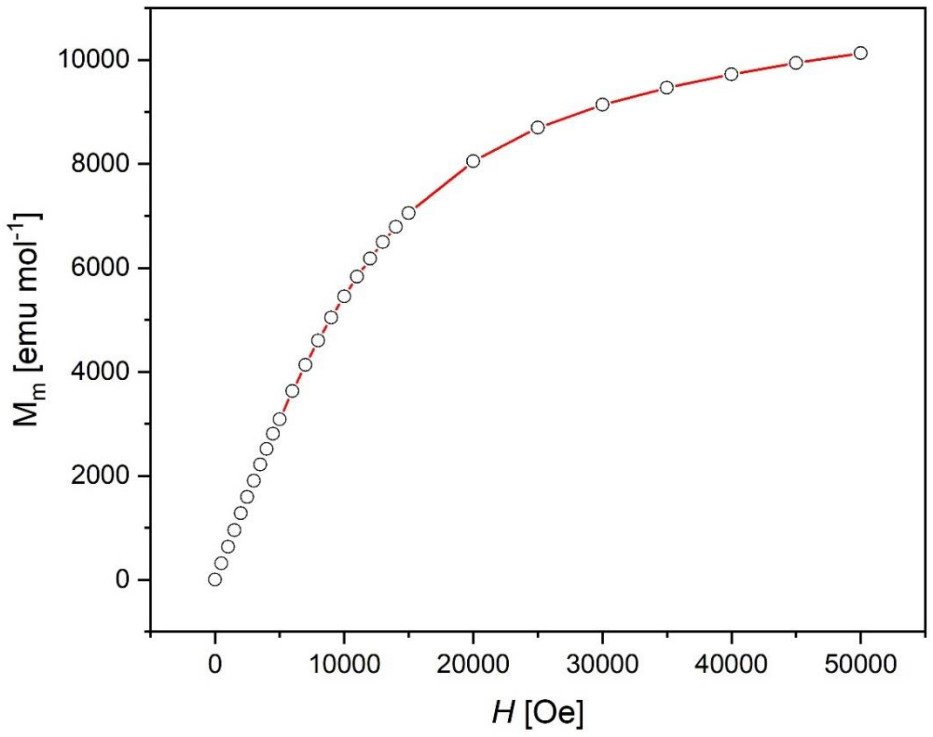

Figure S6. Molar magnetization M_m of **1** between 0 and 5 Tesla at 2 K.

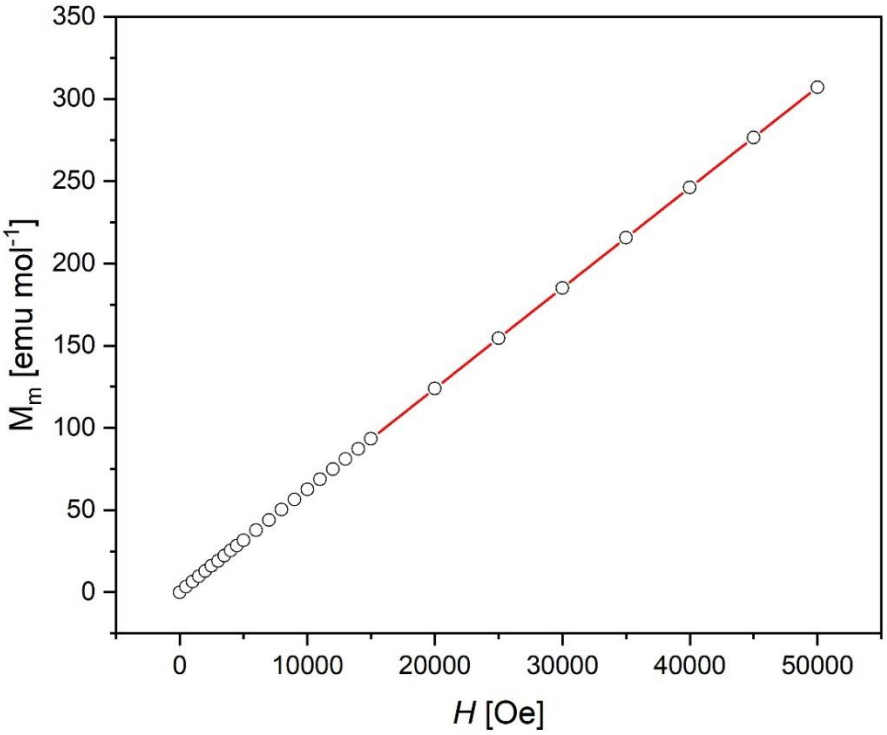

Figure S7. Molar magnetization M_m of **1** between 0 and 5 Tesla at 300 K.

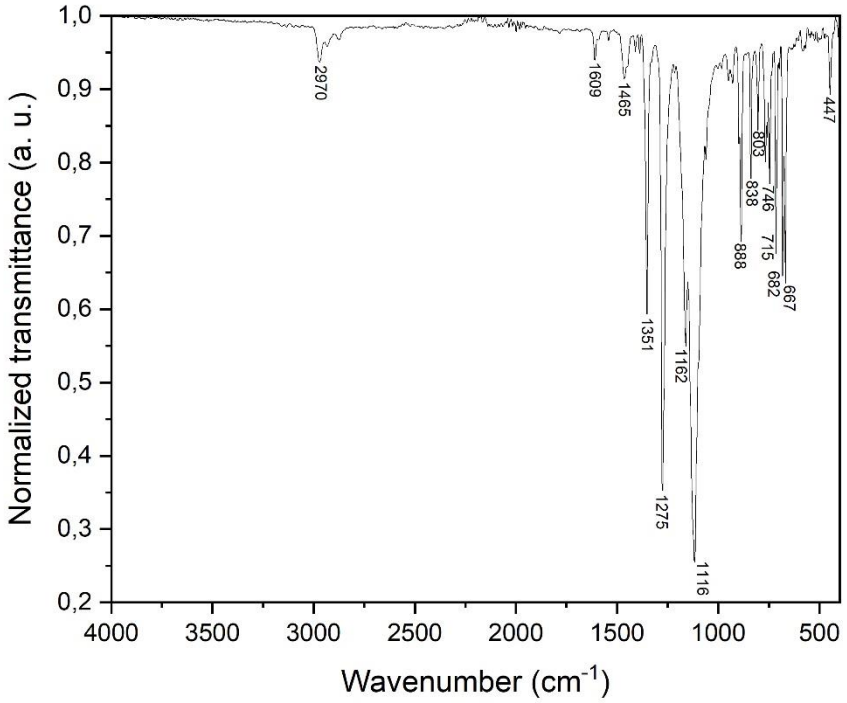

Figure S8. The ATR-IR spectrum of **1**.

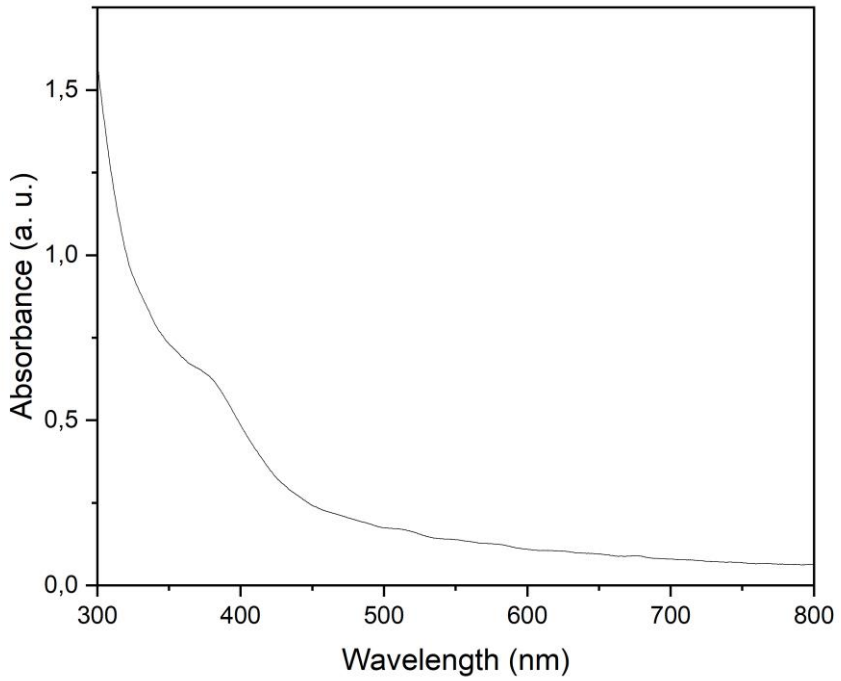

Figure S9. The UV/vis spectrum of **1** as a $1x10^{-3}$ mmol solution in fluorobenzene.

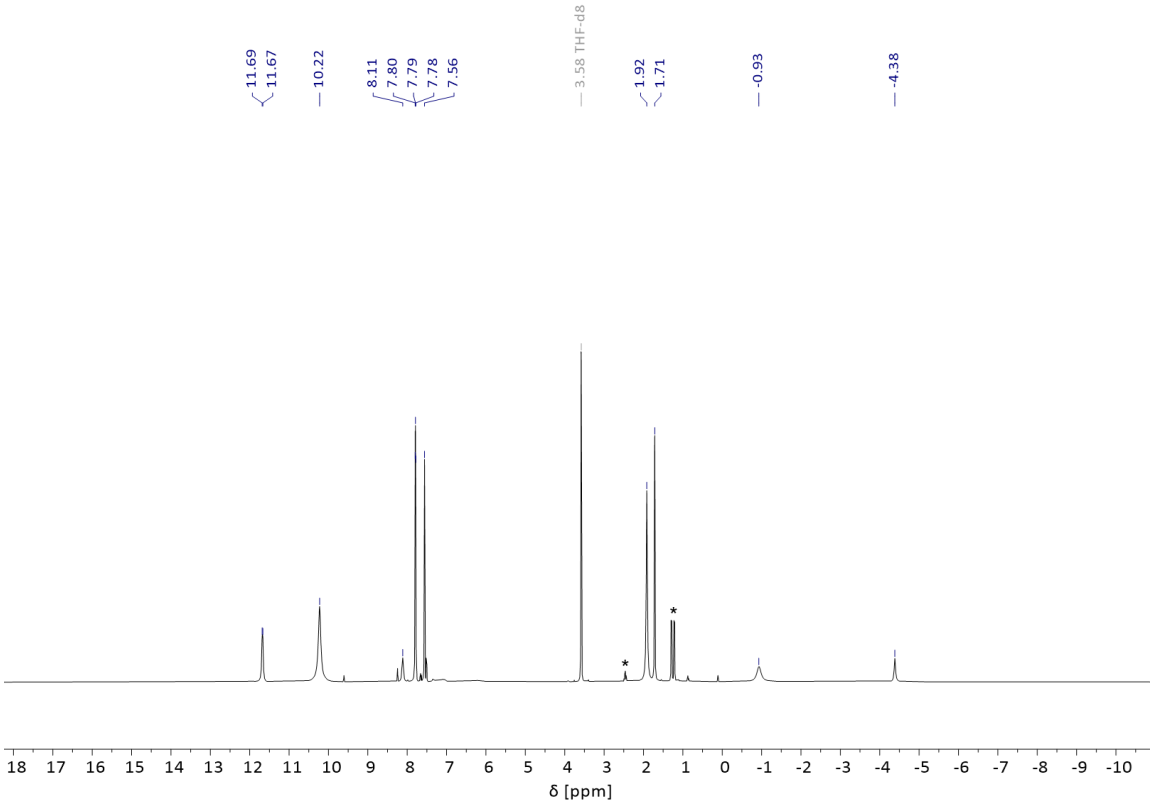

Figure S10. ^{1}H NMR spectrum of **2** as a solution in THF-d^8 at ambient temperature; * indicates small amounts of free ^{Dipp}NHC.

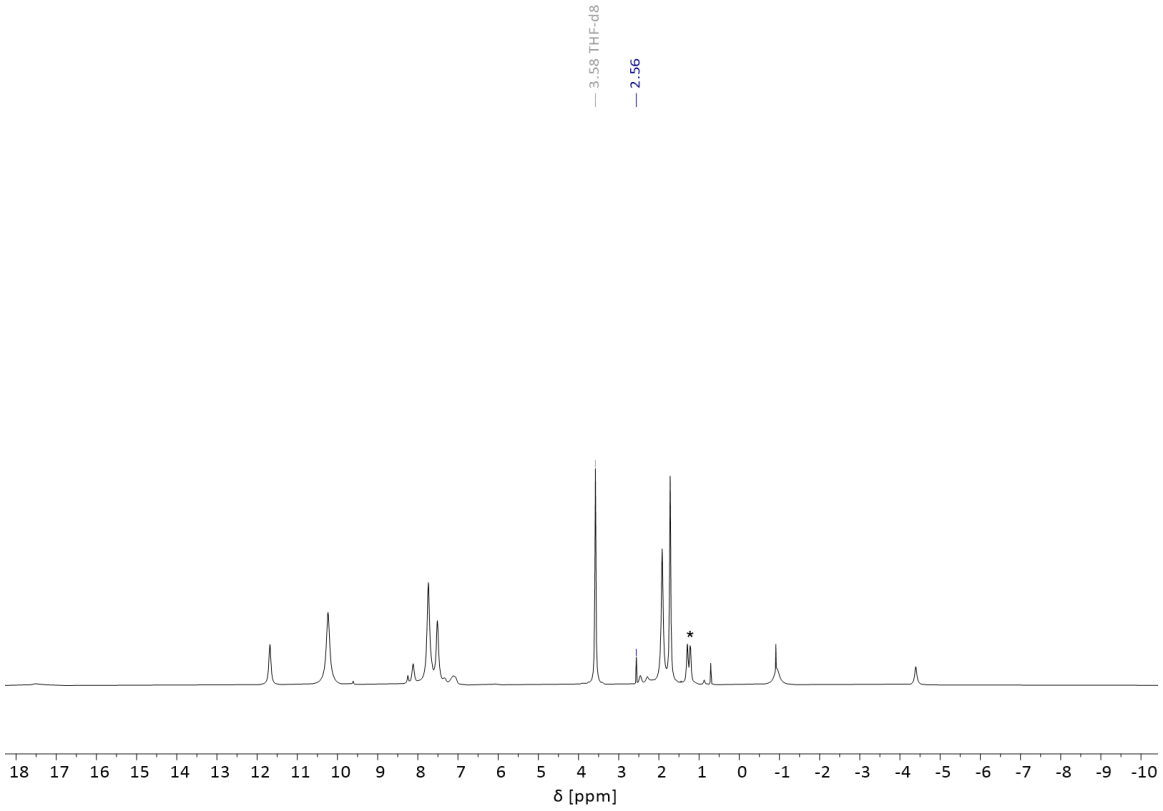

Figure S11. ^{1}H NMR spectrum of **2** as a solution in THF-d^8 at ambient temperature with a THF-d^8 capillary added; * indicates small amounts of free ^{Dipp}NHC.

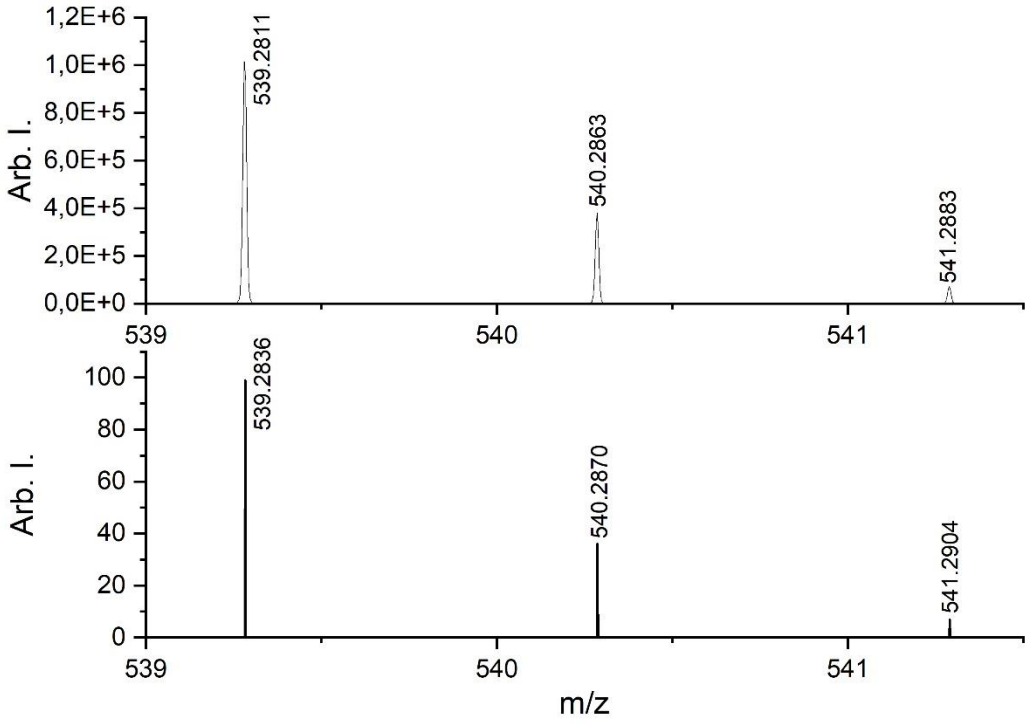

Figure S12. *Top:* Cutout from LIFDI/MS of **2;** *Bottom:* Calculated MS spectrum of [**2**-BAr_4^F]$^+$.

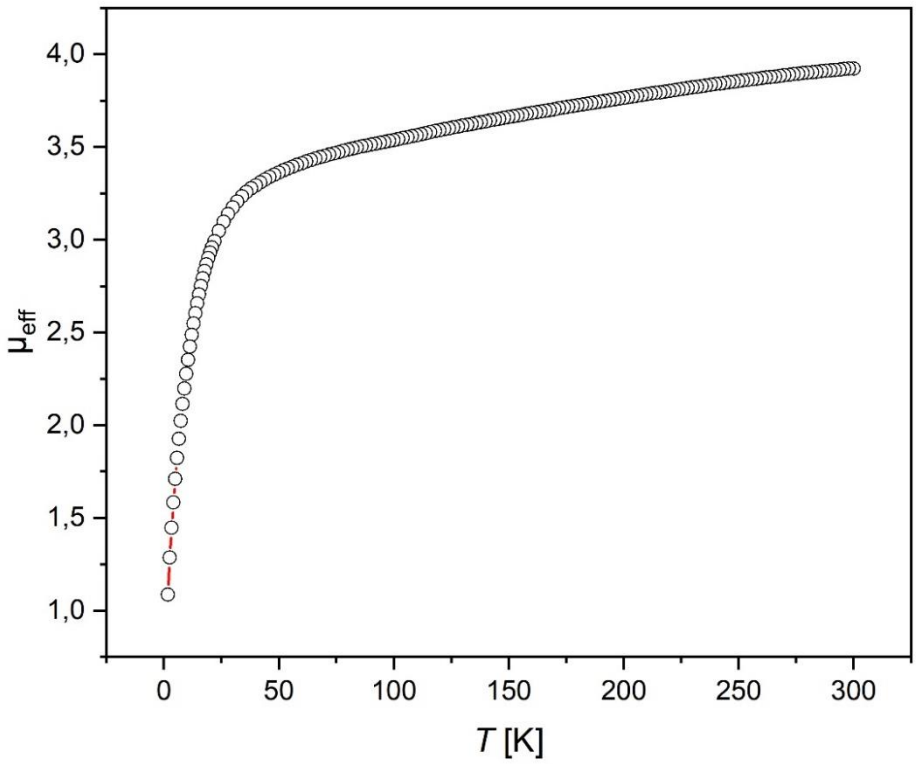

Figure S13. Effective magnetic moment μ_{eff} of crystalline sample of **2** from 1.8 K to 300 K.

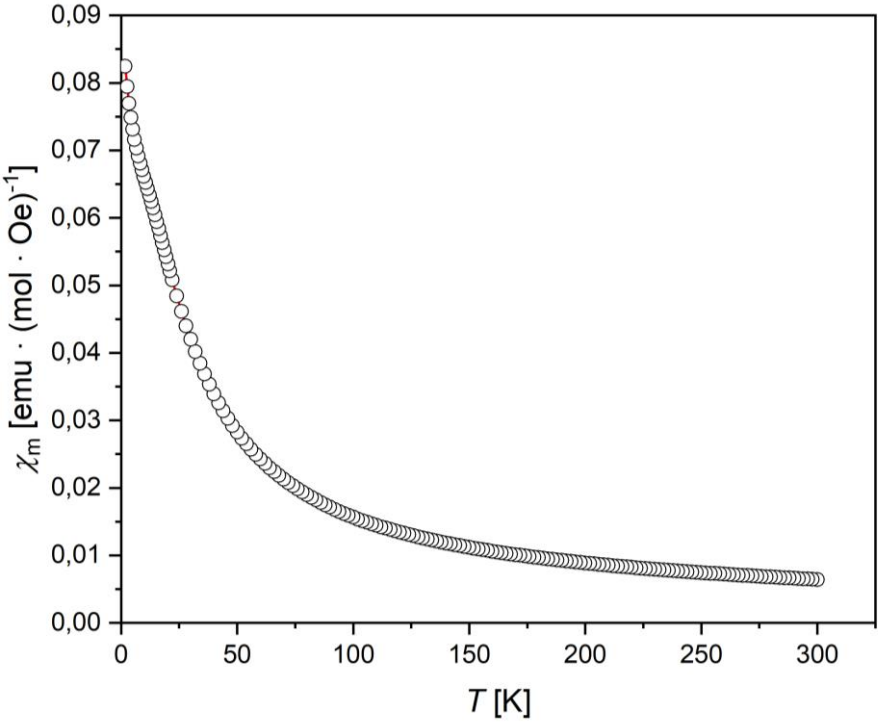

Figure S14. Magnetic susceptibility χ_M of a crystalline sample of **2** from 1.8 K to 300 K.

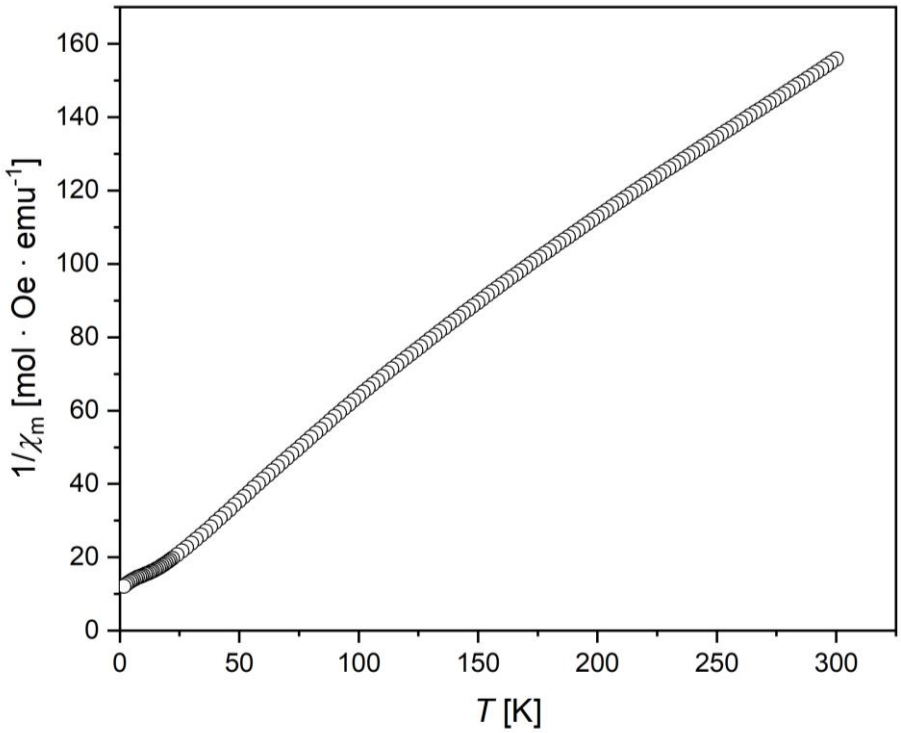

Figure S15. Inverse of the magnetic susceptibility $1/\chi_M$ of a crystalline sample of **2** from 1.8 K to 300 K.

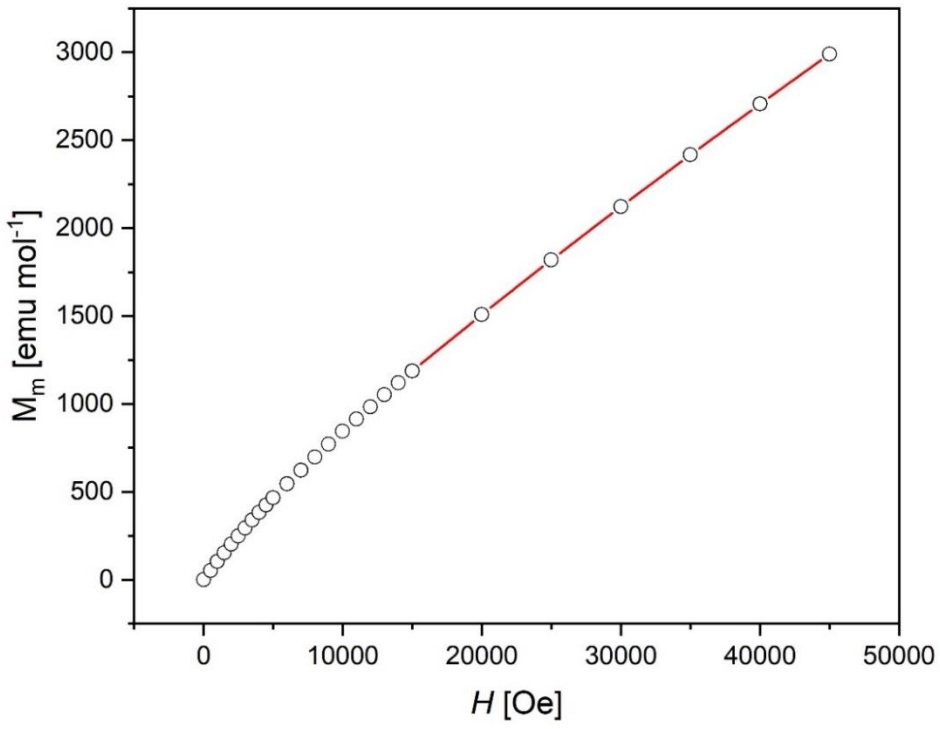

Figure S16. Molar magnetization M_m of **2** between 0 and 5 Tesla at 2 K.

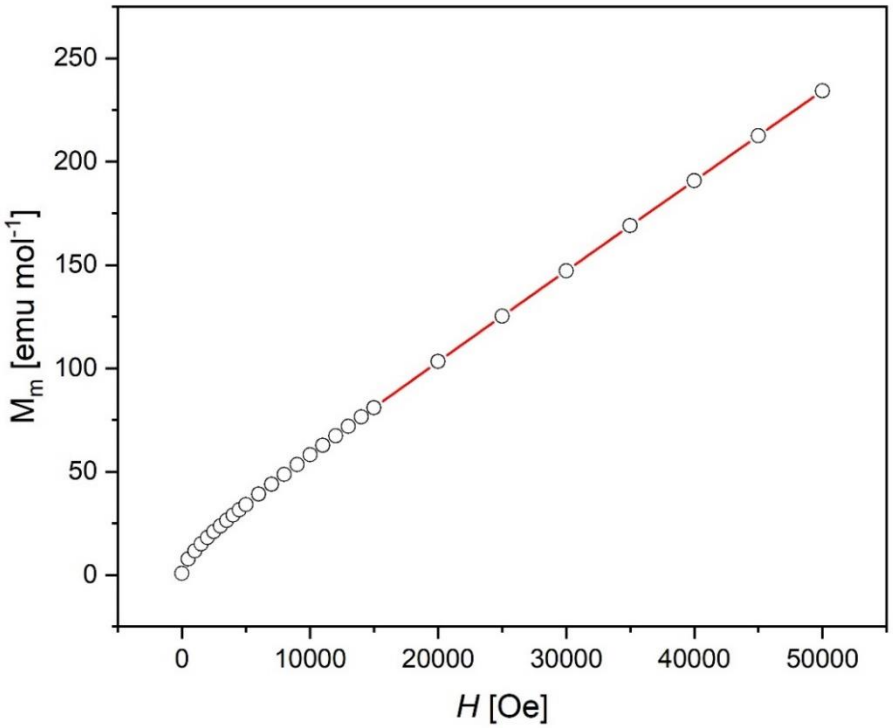

Figure S17. Molar magnetization M_m of **2** between 0 and 5 Tesla at 300 K.

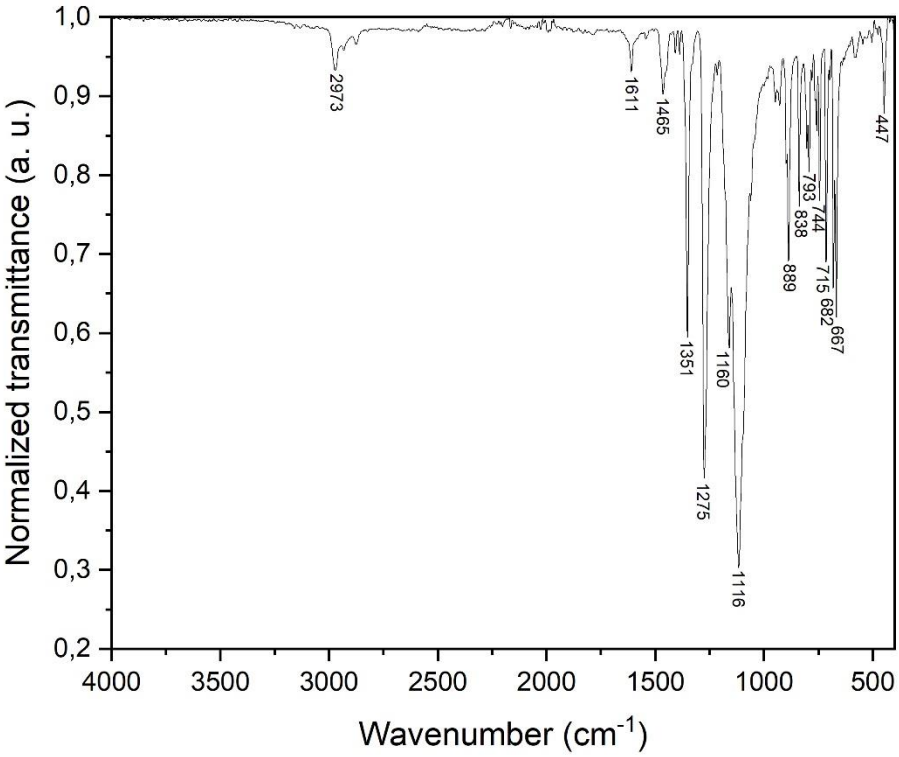

Figure S18. The ATR-IR spectrum of **2**.

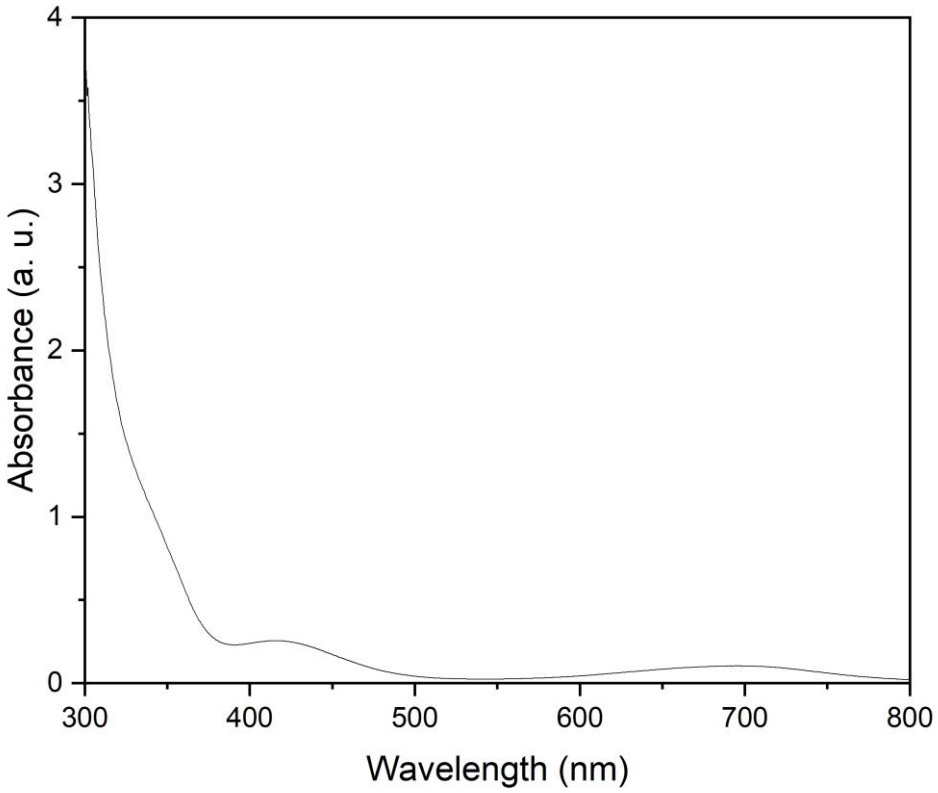

Figure S19. The UV/vis spectrum of **2** as a 1x10^{-3} mmol solution in fluorobenzene.

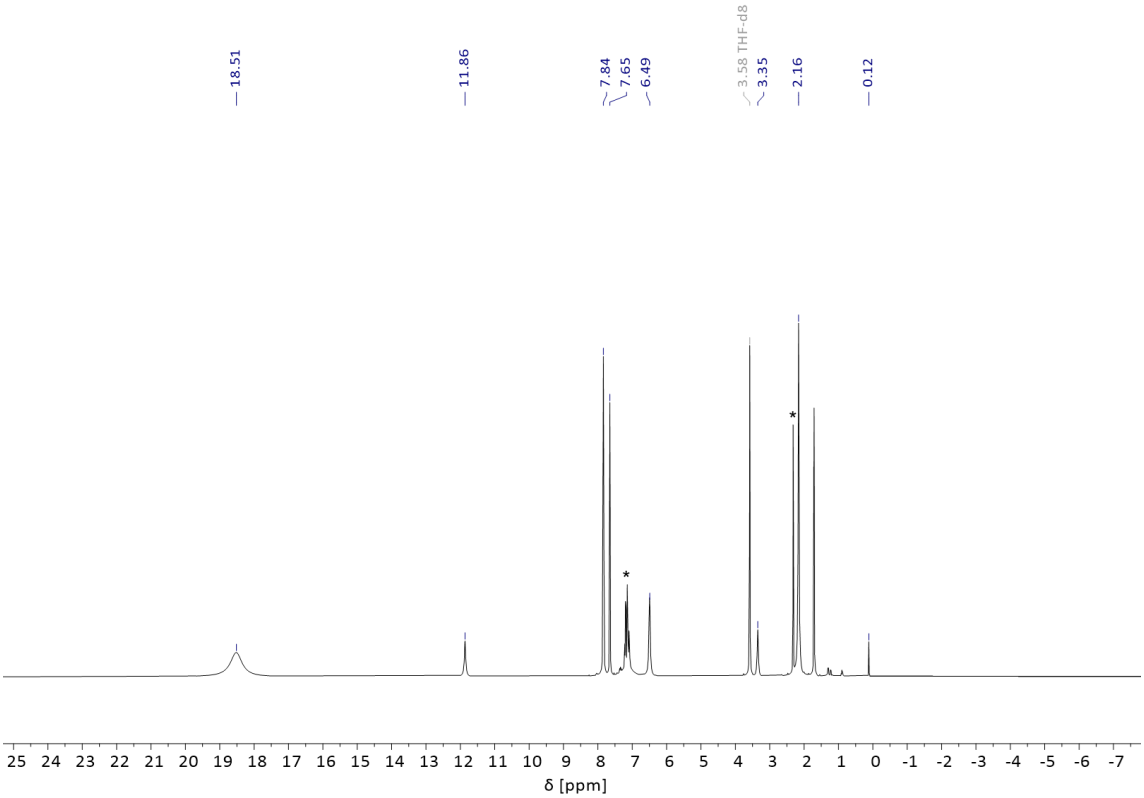

Figure S20. ^{1}H NMR spectrum of **3** as a solution in THF-d^{8} at ambient temperature; * indicates small amounts of free toluene.

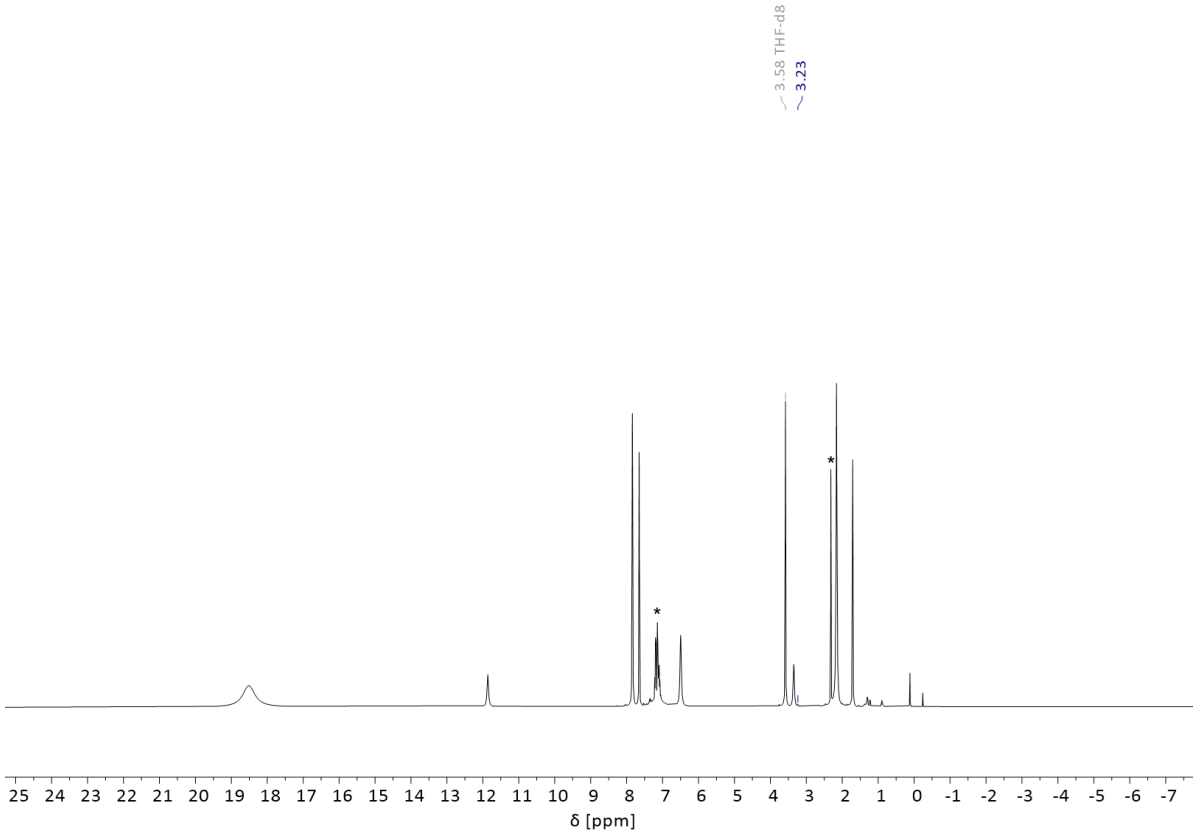

Figure S21. ^{1}H NMR spectrum of **3** as a solution in THF-d^8 at ambient temperature with a THF-d^8 capillary added; * indicates small amounts of free toluene.

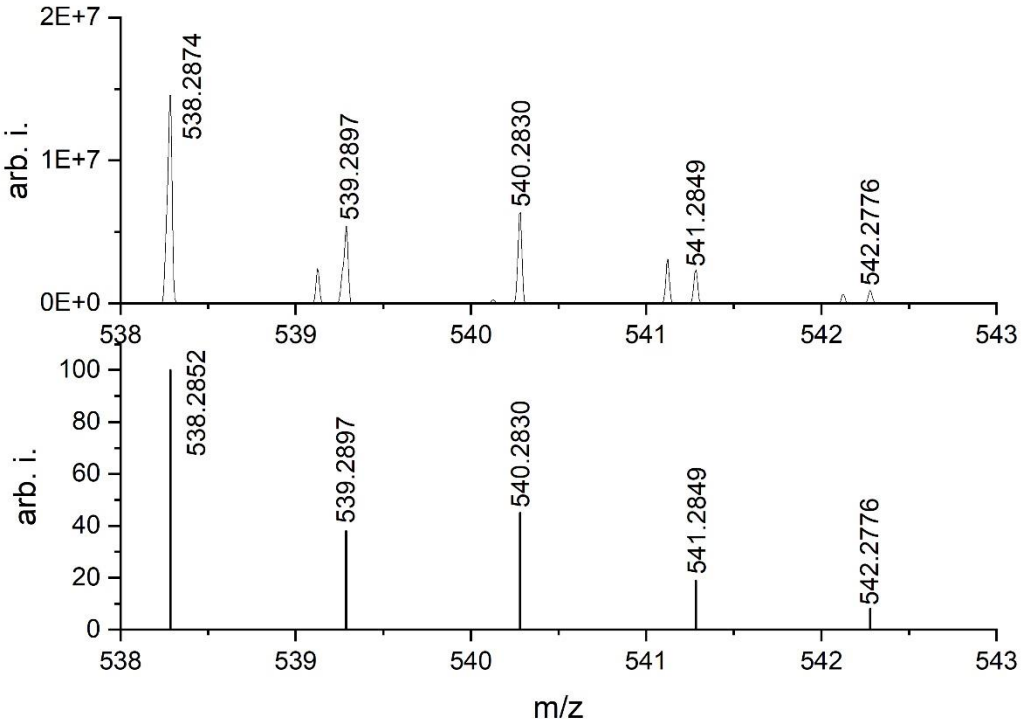

Figure S22. *Top:* Cutout from LIFDI/MS of **3;** *Bottom:* Calculated MS spectrum of [**3**-BAr_4^F]$^+$.

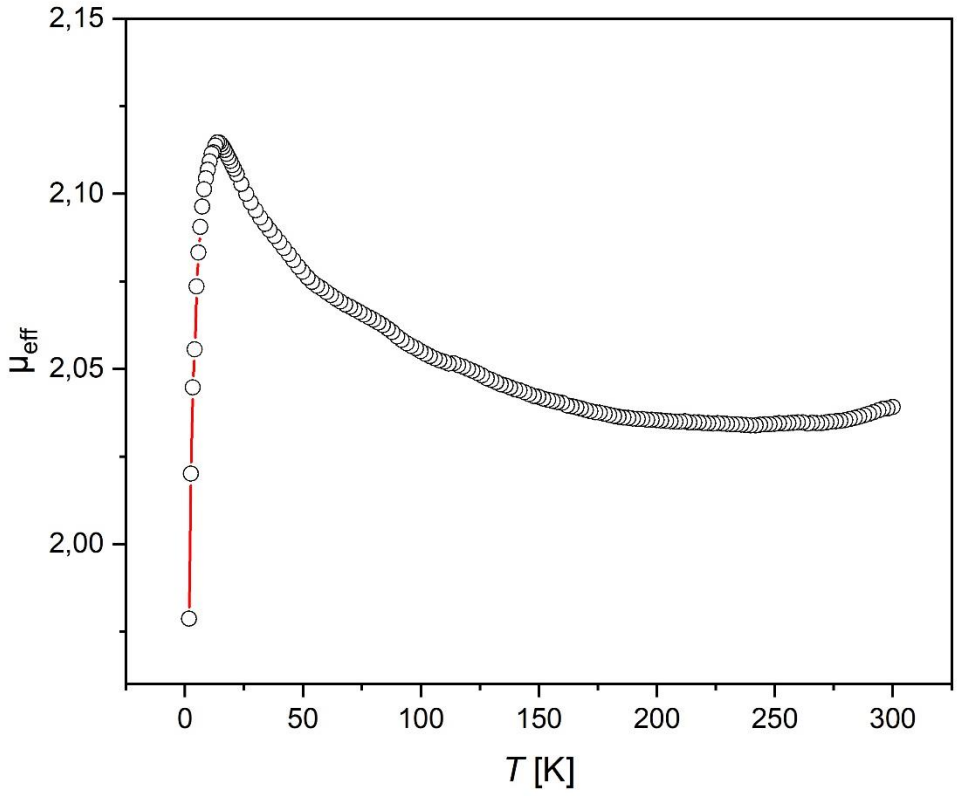

Figure S23. Effective magnetic moment μ_{eff} of crystalline sample of **3** from 1.8 K to 300 K.

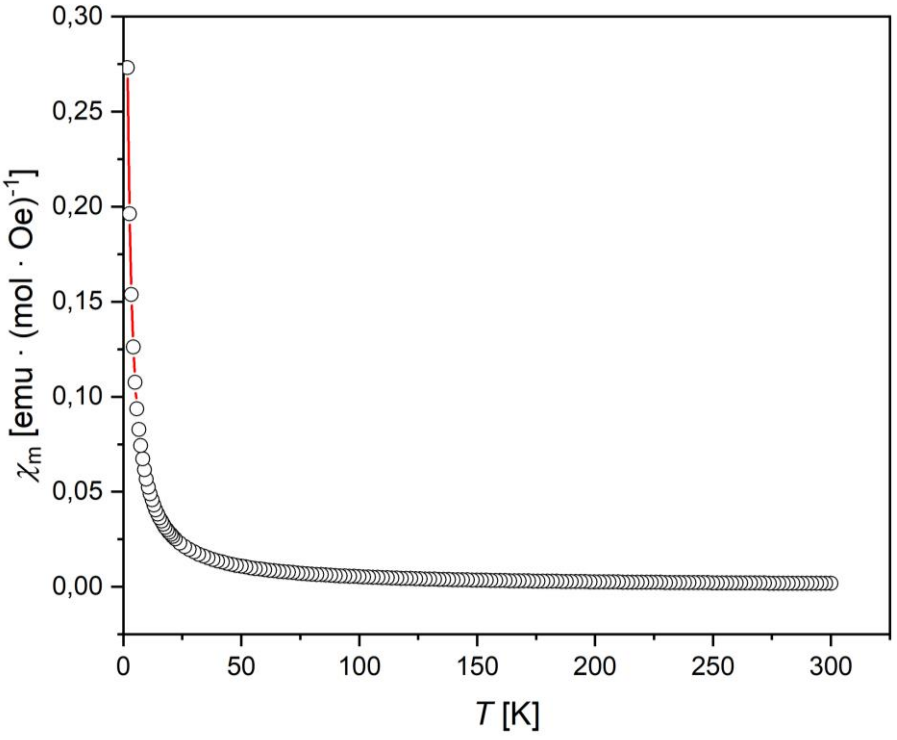

Figure S24. Magnetic susceptibility χ_M of a crystalline sample of **3** from 1.8 K to 300 K.

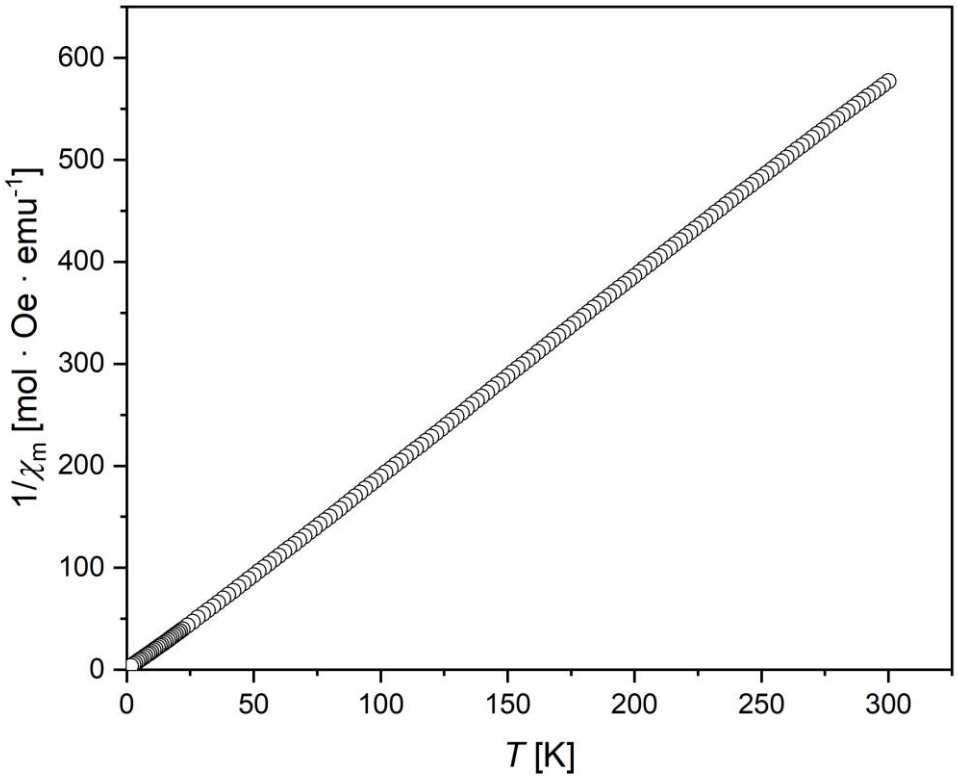

Figure S25. Inverse of the magnetic susceptibility $1/\chi_M$ of a crystalline sample of **3** from 1.8 K to 300 K.

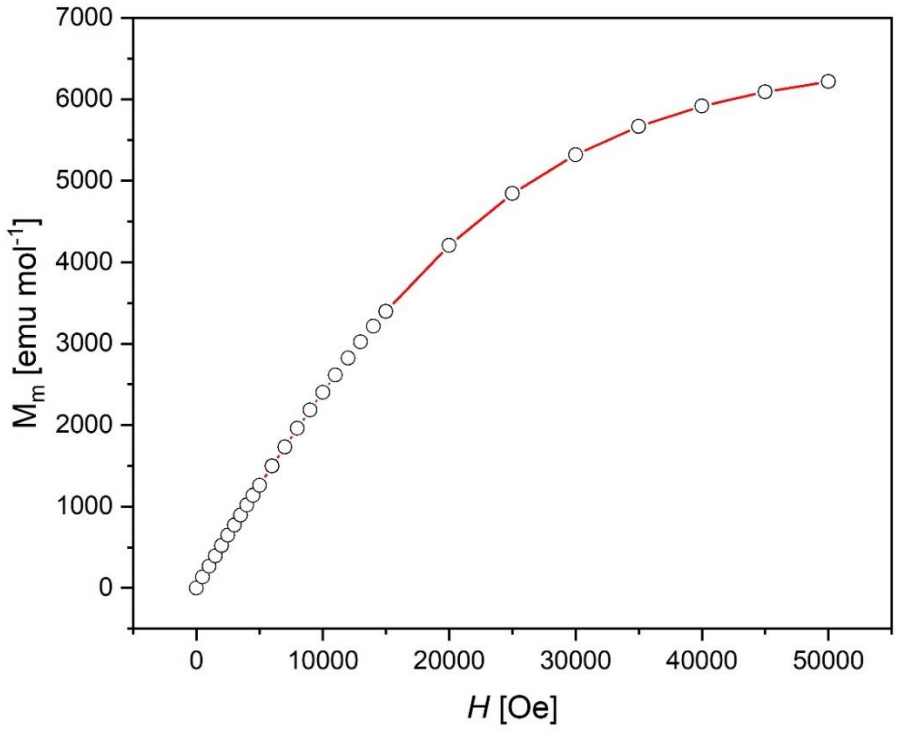

Figure S26. Molar magnetization M_m of **3** between 0 and 5 Tesla at 2 K.

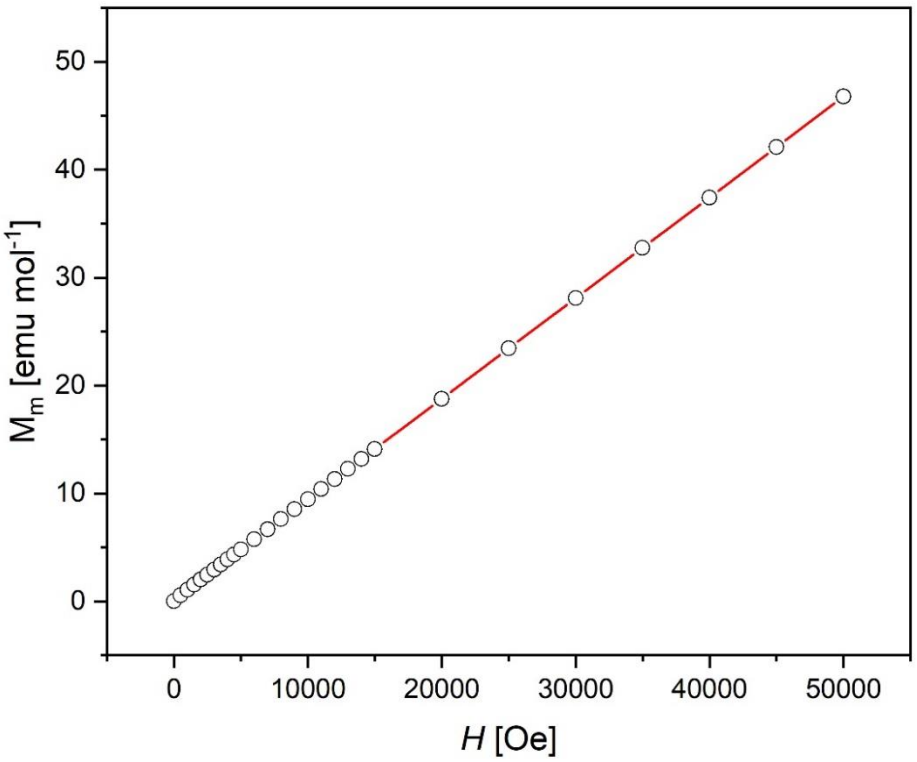

Figure S27. Molar magnetization M_m of **3** between 0 and 6 Tesla at 300 K.

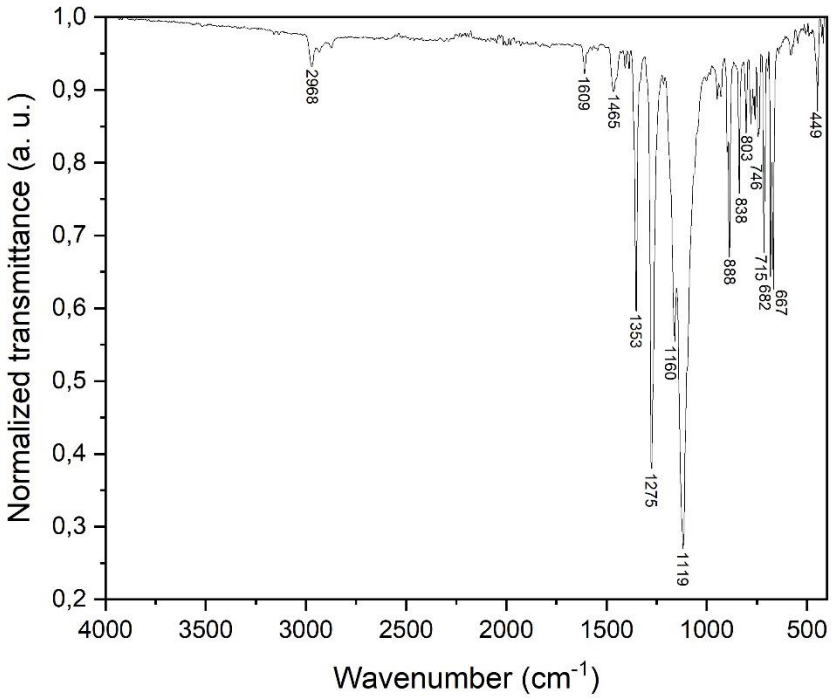

Figure S28. The ATR-IR spectrum of **3**.

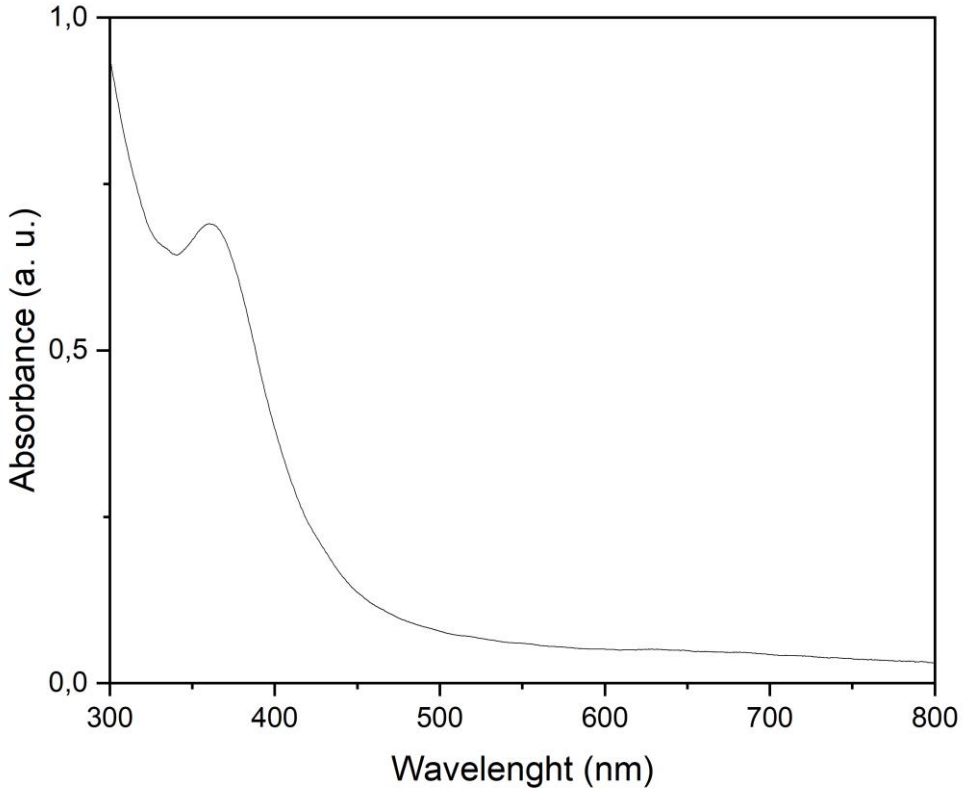

Figure S29. The UV/vis spectrum of **3** as a $3x10^{-4}$ mmol solution in fluorobenzene.

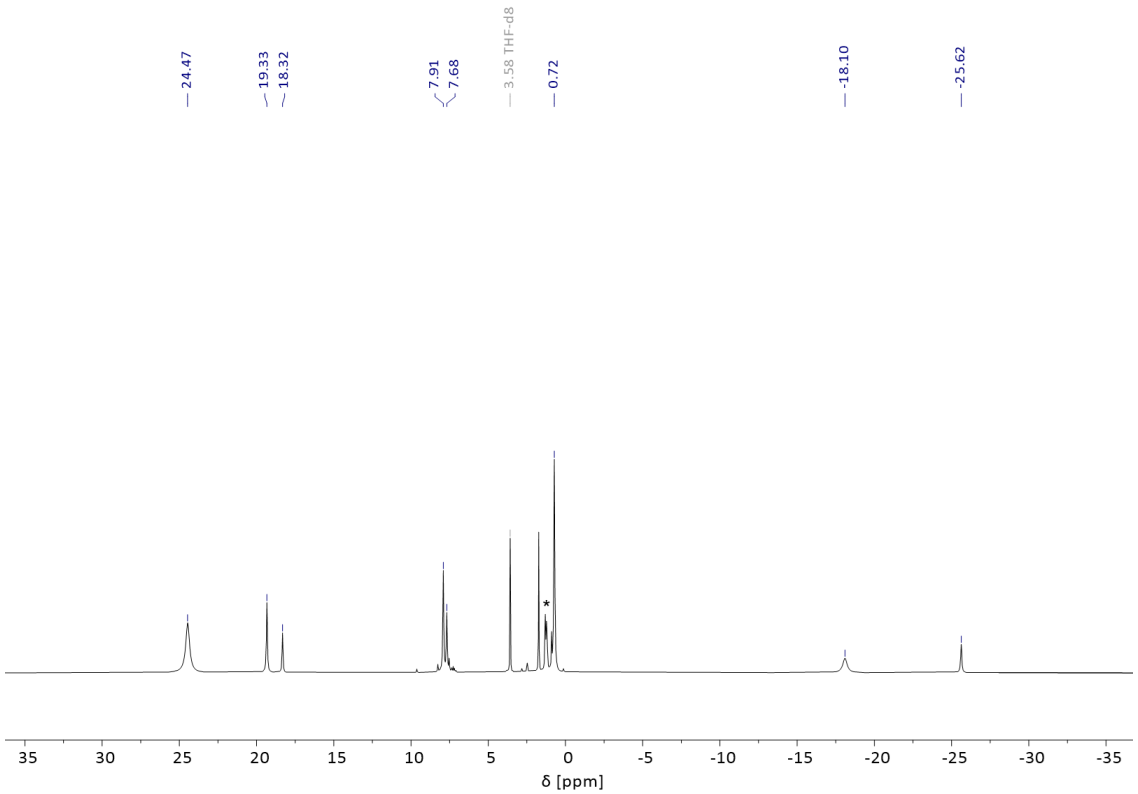

Figure S30. ^{1}H NMR spectrum of **4** as a solution in THF-d^8 at ambient temperature; * indicates small amounts of free ^{Dipp}NHC.

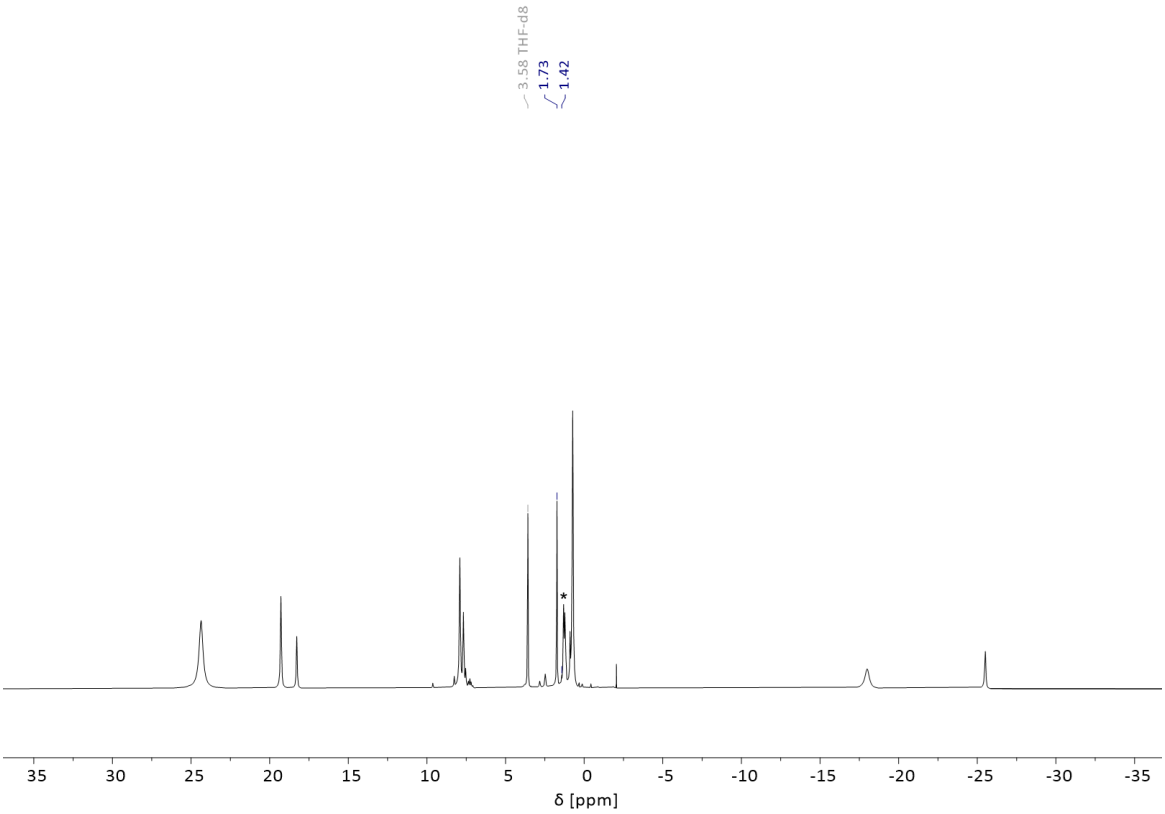

Figure S31. ^{1}H NMR spectrum of **4** as a solution in THF-d^8 at ambient temperature with a THF-d^8 capillary added; * indicates small amounts of free DippNHC.

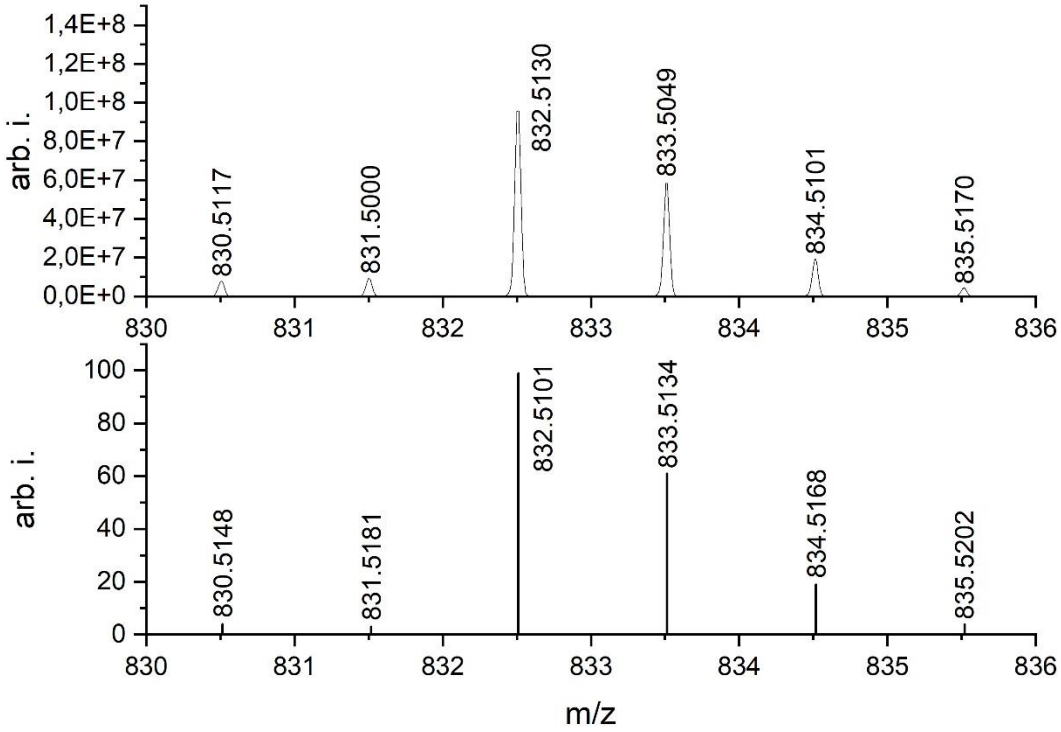

Figure S32. *Top:* Cutout from LIFDI/MS of **4;** *Bottom:* Calculated MS spectrum of [**4**-BAr_4^F]$^+$.

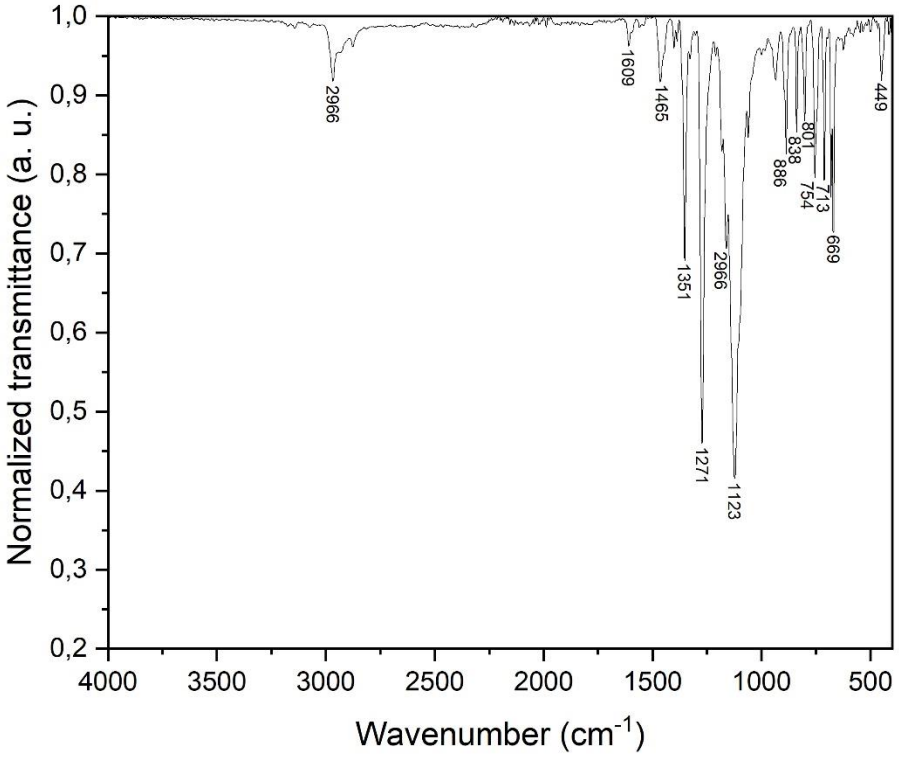

Figure S33. The ART-IR spectrum of **4**.

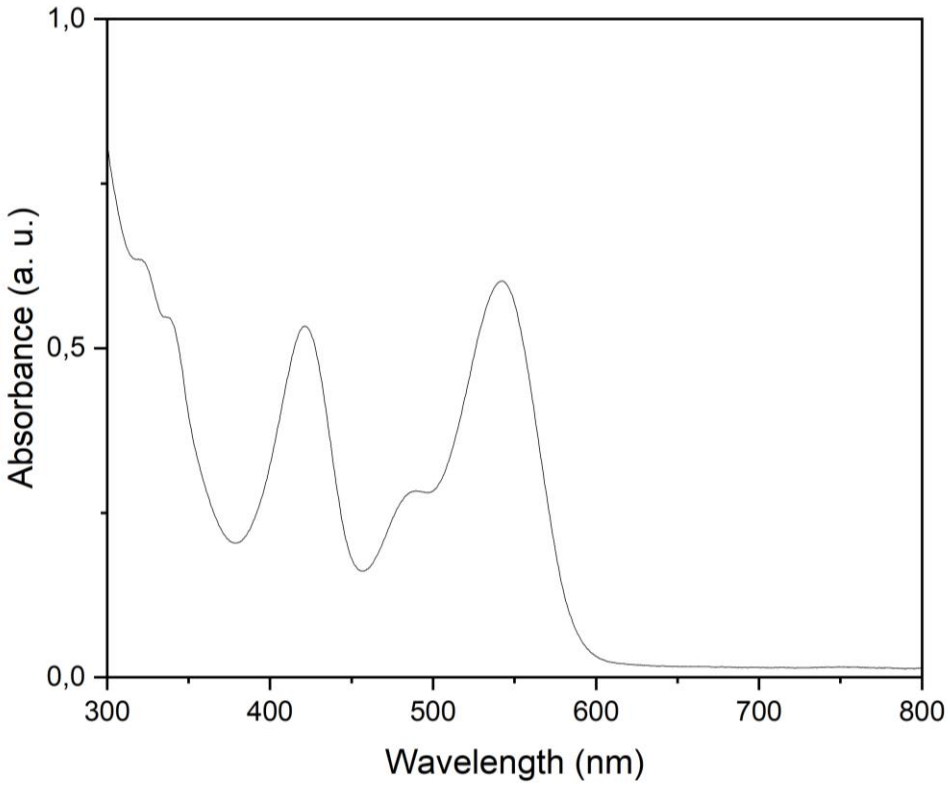

Figure S34. The UV/vis spectrum of **4** as a $5x10^{-4}$ mmol solution in fluorobenzene.

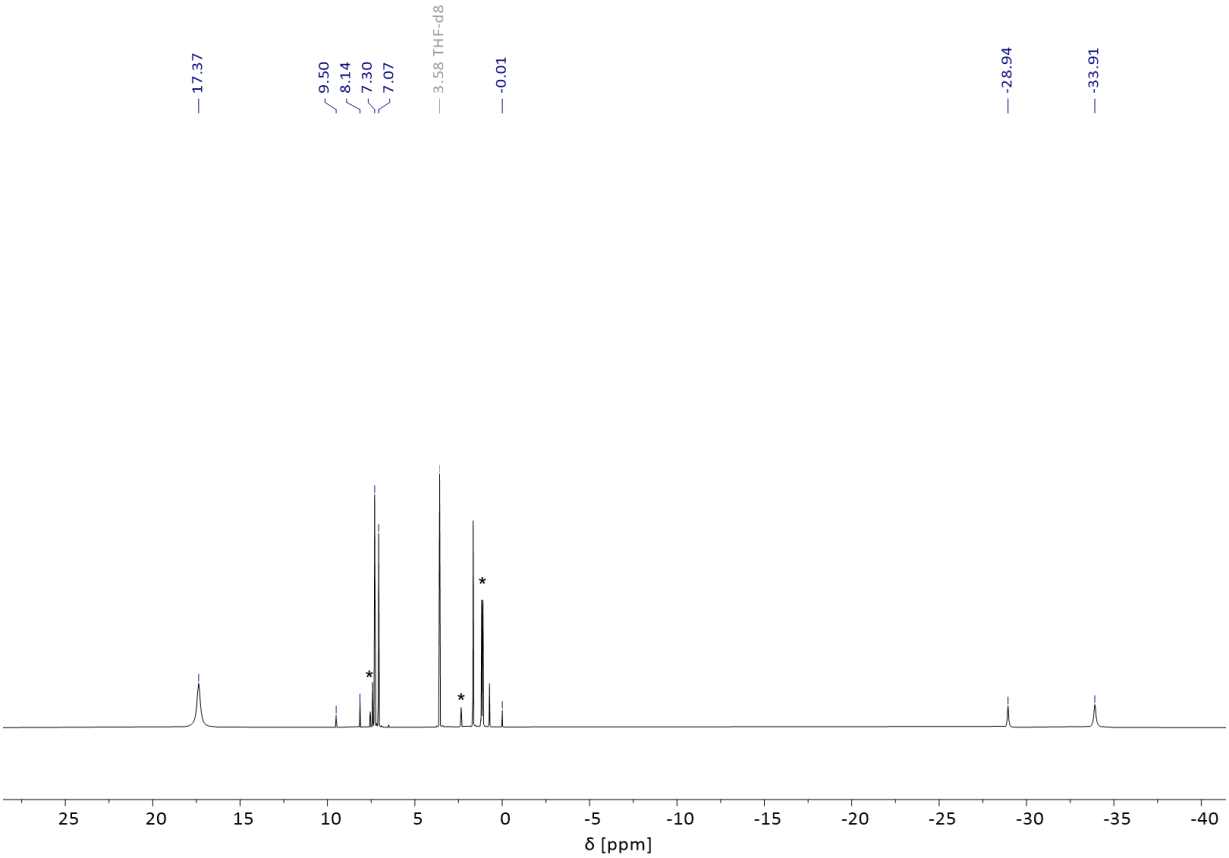

Figure S35. ^{1}H NMR spectrum of **5** as a solution in THF-d^8 at ambient temperature; * indicates small amounts of free ^{Dipp}NHC.

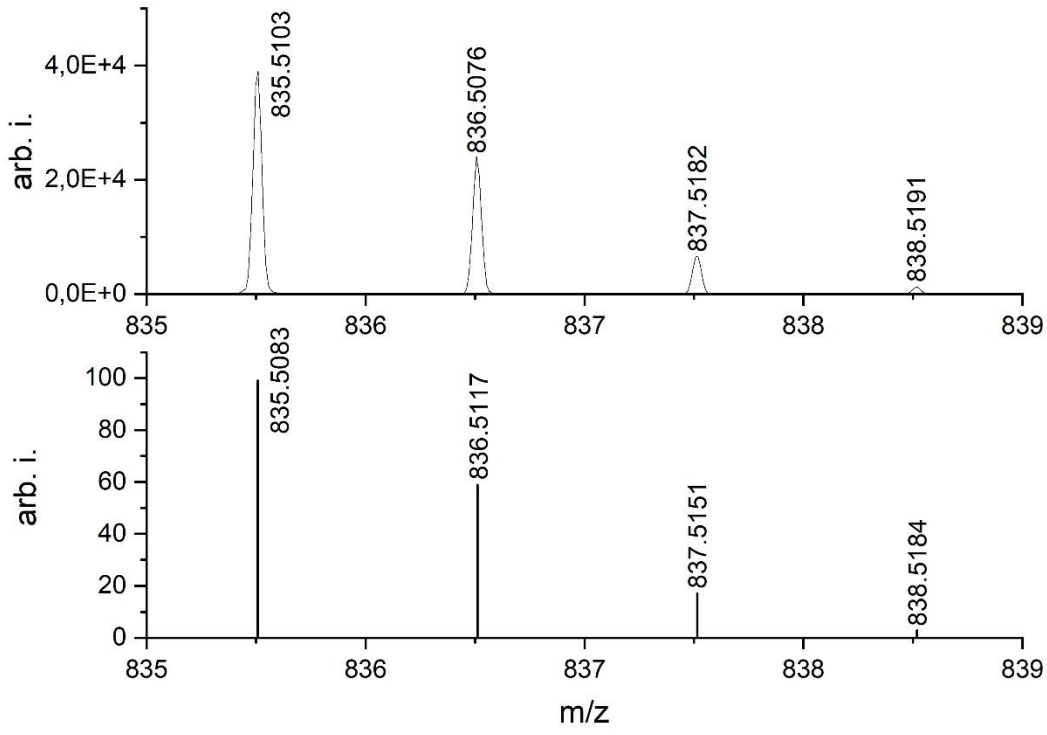

Figure S36. *Top:* Cutout from LIFDI/MS of **5;** *Bottom:* Calculated MS spectrum of [**5**-BAr$^{F}{}_4$]$^+$.

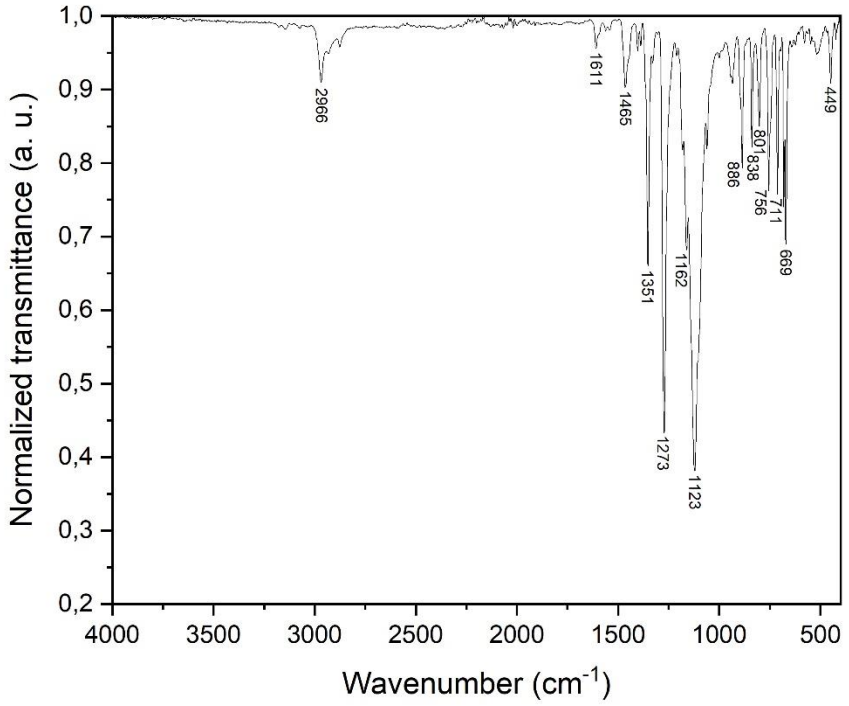

Figure S37. The ART-IR spectrum of **5**.

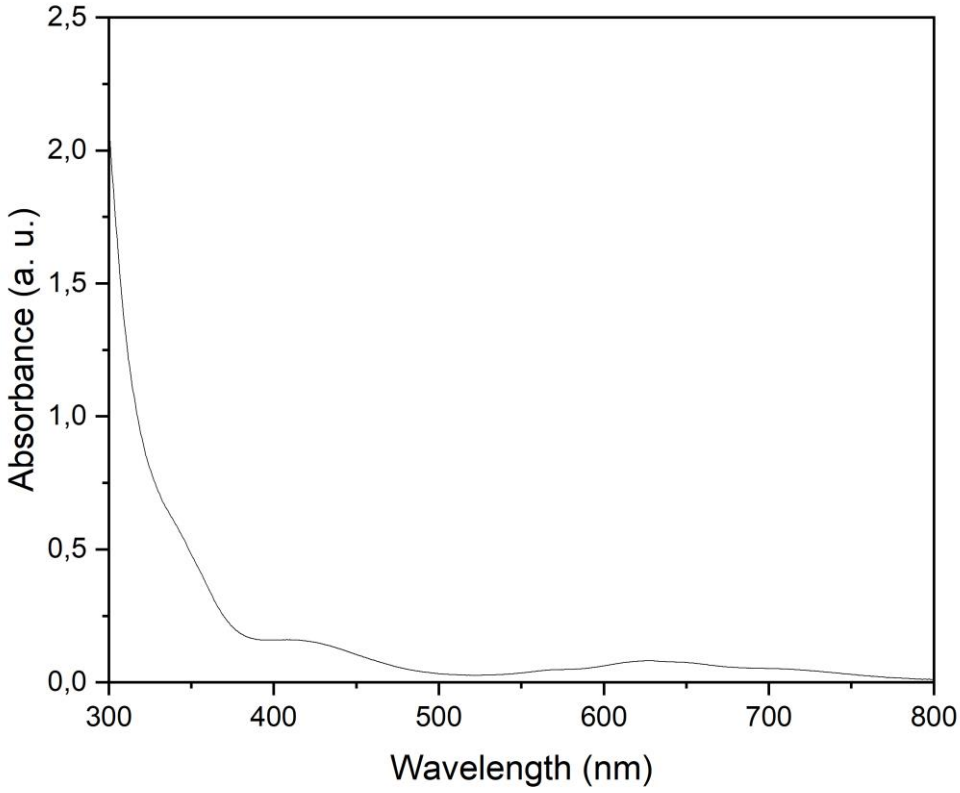

Figure S38. The UV/vis spectrum of **5** as a $5x10^{-4}$ mmol solution in fluorobenzene.

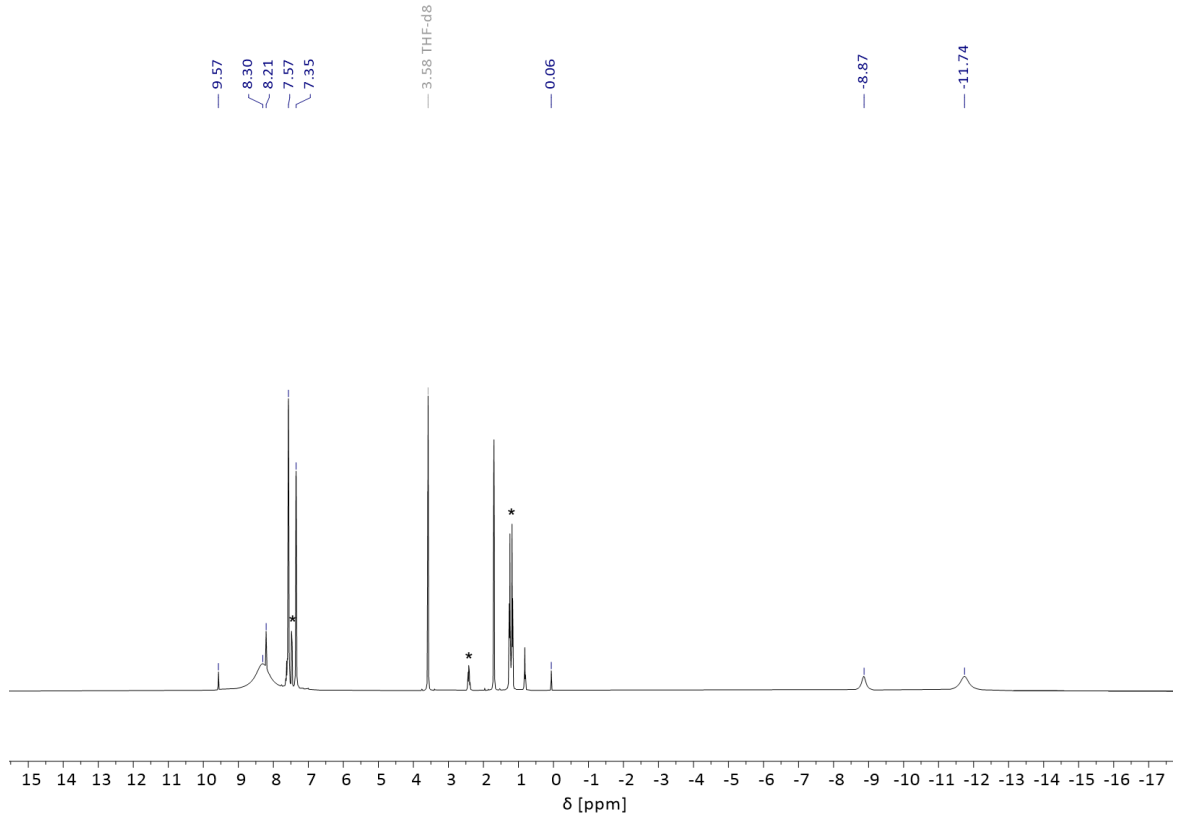

Figure S39. ^{1}H NMR spectrum of **6** as a solution in THF-d^8 at ambient temperature; * indicates small amounts of free ^{Dipp}NHC.

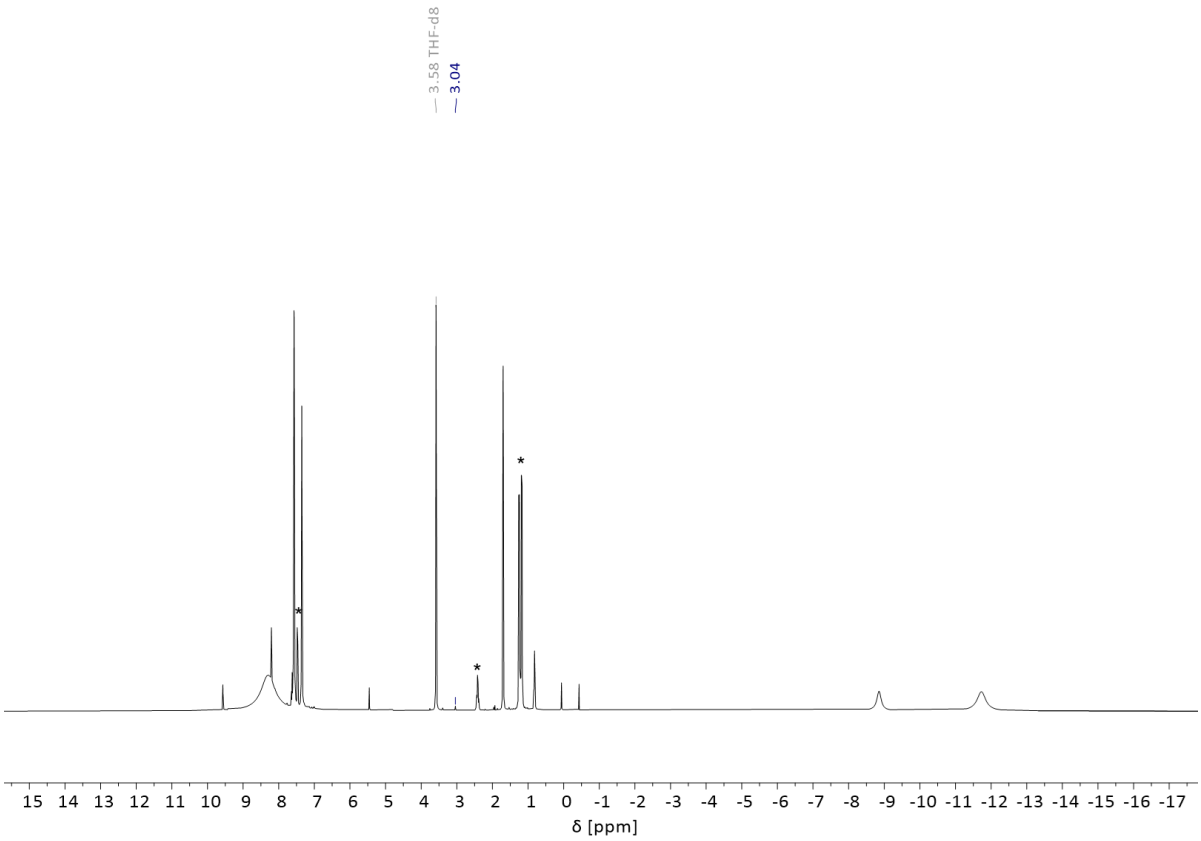

Figure S40. ^{1}H NMR spectrum of **6** as a solution in THF-d^8 at ambient temperature with a THF-d^8 capillary added; * indicates small amounts of free DippNHC.

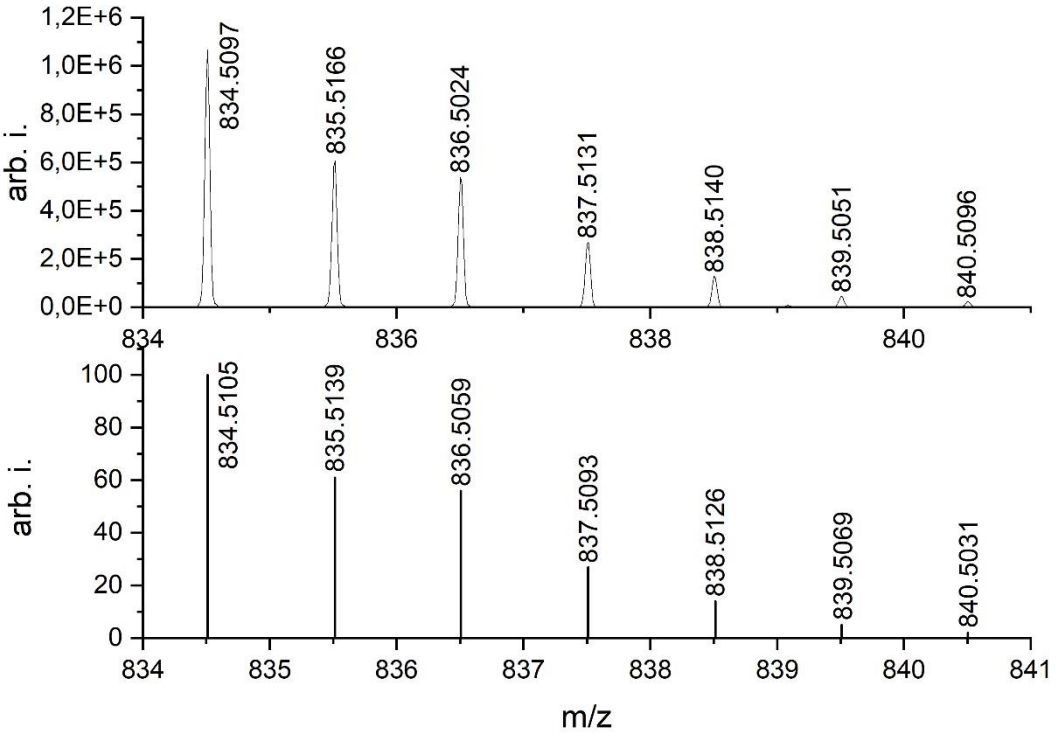

Figure S41. *Top:* Cutout from LIFDI/MS of **6;** *Bottom:* Calculated MS spectrum of [**6**-BAr$^{F}{}_{4}$]$^{+}$.

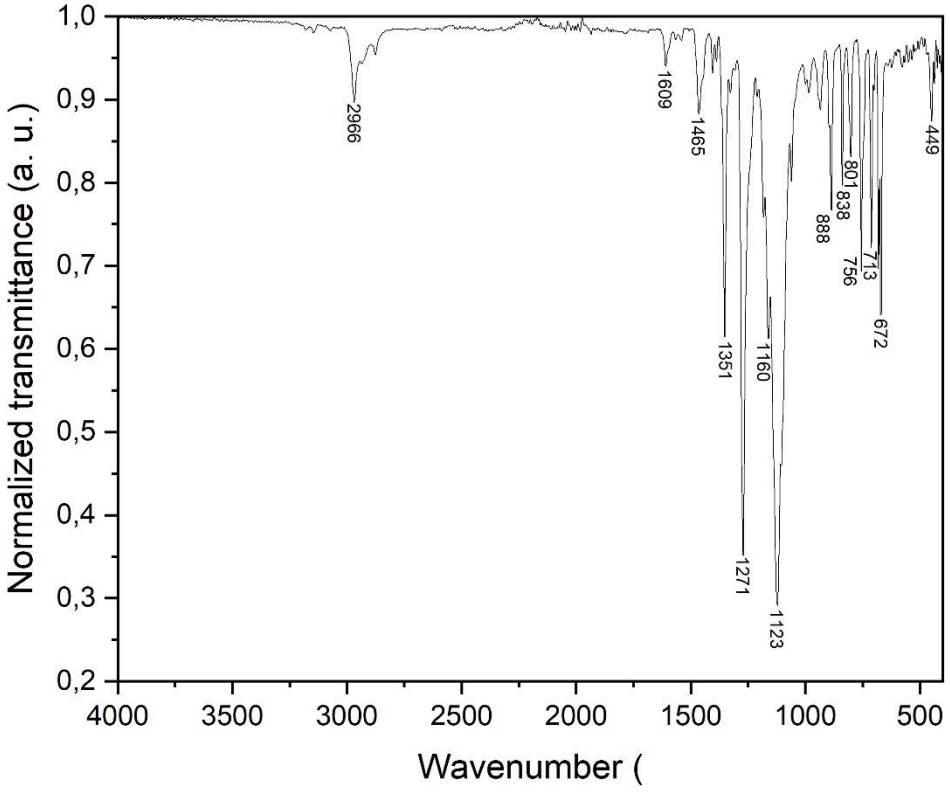

Figure S42. The ART-IR spectrum of **6**.

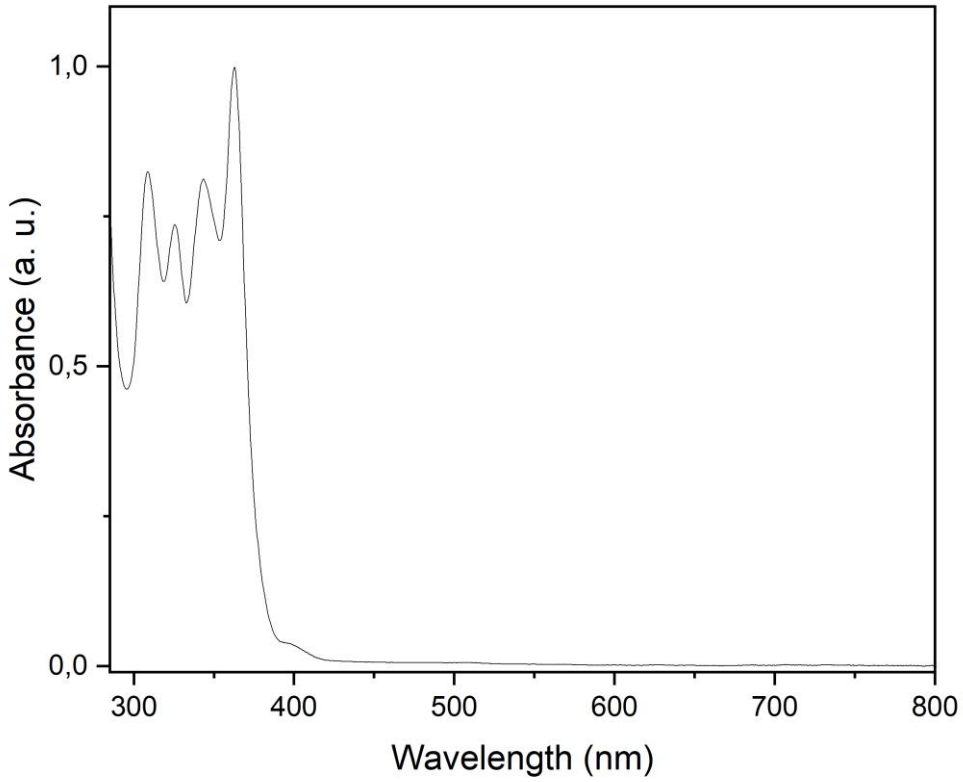

Figure S43. The UV/vis spectrum of **6** as a $2x10^{-4}$ mmol solution in fluorobenzene.

2. X-ray crystallographic details

Single crystals of **1**-**6** suitable for X-ray structural analysis were mounted in perfluoroalkyl ether oil on a nylon loop and positioned in a 150 K cold N_2 gas stream. Data collection was performed with a STOE StadiVari diffractometer (MoKα radiation) equipped with a DECTRIS PILATUS 300K detector. Structures were solved by Direct Methods (SHELXS-97) and refined by full-matrix least-squares calculations against F^2 (SHELXL-2018). The positions of the hydrogen atoms were calculated and refined using a riding model. All non-hydrogen atoms were treated with anisotropic displacement parameters. Crystal data, details of data collections, and refinements for all structures can be found in their CIF files, which are available free of charge via www.ccdc.cam.ac.uk/data_request/cif, and are summarized in Table S1.

Responses to CheckCIF A and B Alerts:

Compound **1**:

PLAT220_ALERT_2_B NonSolvent Resd 1 F Ueq(max)/Ueq(min) Range
10.0 Ratio

This is due to disorder in the BAr^F_4 anion, which has been modelled.

Compound **2**:

PLAT213_ALERT_2_B Atom F5 has ADP max/min Ratio .....
4.1 prolat
PLAT213_ALERT_2_B Atom F16 has ADP max/min Ratio .....
4.2 prolat
PLAT220_ALERT_2_B NonSolvent Resd 1 F Ueq(max)/Ueq(min) Range
6.4 Ratio

As above, these are all due to disorder in the BAr^F_4 anion, which has been modelled.

Compound **4:**

PLAT214_ALERT_2_A Atom F13A (Anion/Solvent) ADP max/min Ratio
10.9 prolat

This is due to particularly bad disorder in one CF_3 group of the BAr^F_4 anion, which could not be completely modelled. This, however, does not effect the overall quality of the data (R(int) = 3.85%, R1 = 7.72%).

PLAT201_ALERT_2_B Isotropic non-H Atoms in Main Residue(s) .....
3 Report: C22A C23A C24A

These are C-atoms in part 2 of a modelled disordered carbene.

PLAT221_ALERT_2_B Solv./Anion Resd 2 F Ueq(max)/Ueq(min) Range
10.0 Ratio

As above, this is all due to disorder in the BAr^F_4 anion, which has been modelled.

PLAT910_ALERT_3_B Missing # of FCF Reflection(s) Below Theta(Min).
17 Note

As the data completeness is high (99.9%), and the quality good, this does not effect the publishability of this data set.

Compound **5**:

PLAT220_ALERT_2_B NonSolvent Resd 1 F Ueq(max)/Ueq(min) Range
6.7 Ratio
PLAT220_ALERT_2_B NonSolvent Resd 2 C Ueq(max)/Ueq(min) Range
10.0 Ratio

As above, these are both due to disorder in the BAr^F_4 anion, which has been modelled.

Compound **6**:

PLAT220_ALERT_2_B NonSolvent Resd 2 C Ueq(max)/Ueq(min) Range 10.0 Ratio
PLAT234_ALERT_4_B Large Hirshfeld Difference C52 --C53 . 0.26 Ang.
As above, these are both due to disorder in the BAr^F_4 anion, which has been modelled.

PLAT242_ALERT_2_B Low 'MainMol' Ueq as Compared to Neighbors of C13 Check
This is due to disorder in one iPr group of a carbene.

Table S1. Summary of X-ray crystallographic data for **1**, **2**, and **3**.

	1	**2**	**3**
empirical form.	$C_{66}H_{56}BF_{24}FeN_2$	$C_{66}H_{56}BF_{24}CoN_2$	$C_{66}H_{56}BF_{24}NiN_2$
formula wt	1399.78	1402.86	1402.64
crystal syst.	monoclinic	monoclinic	monoclinic
space group	*P2₁/c*	*P-1*	*P-1*
a (Å)	13.028(3)	12.970(3)	12.960(3)
b (Å)	19.334(4)	19.245(4)	19.240(4)
c (Å)	25.637(5)	25.726(5)	25.710(5)
α (deg.)	90	90	90
β (δεγ)	101.28(3)	101.04(3)	101.10(3)
γ (deg.)	90	90	90
vol (Å^3)	6333(2)	6302(2)	6291(2)
Z	4	4	4
ρ(calc) (g.cm^{-3})	1.468	1.478	1.481
μ (mm^{-1})	0.352	0.386	0.423
F(000)	2852	2856	2860
T (K)	150(2)	150(2)	150(2)
reflns collect.	35364	44865	44810
unique reflns	12430	12349	12355
R_{int}	0.0615	0.0389	0.0542
R1 [$I>2\sigma(I)$]	0.0577	0.0582	0.0634
*w*R2 (all data)	0.1333	0.1124	0.0979
CCDC No.	2377592	2377593	2377594

Table S2. Summary of X-ray crystallographic data for **4**, **5**, and **6**.

	4	**5**	**6**
empirical form.	$C_{86}H_{84}BFeF_{24}N_4$	$C_{86}H_{84}BCoF_{24}N_4$	$C_{86}H_{84}BNiF_{24}N_4$
formula wt	1696.23	1699.31	1699.09
crystal syst.	monoclinic	monoclinic	monoclinic
space group	$P2_1/n$	$P2_1/n$	$P2_1/n$
a (Å)	16.648(3)	16.638(3)	16.690(3)
b (Å)	28.616(6)	28.489(6)	28.580(6)
c (Å)	17.924(4)	17.907(4)	17.900(4)
α (deg.)	90	90	90
β ($\delta\varepsilon\gamma$)	90.43(3)	90.44(3)	90.40(3)
γ (deg.)	90	90	90
vol (Å^3)	8539(3)	8487(3)	8538(3)
Z	4	4	4
ρ(calc) (g.cm^{-3})	1.319	1.330	1.322
μ (mm^{-1})	0.274	0.300	0.325
F(000)	3500	3504	3508
T (K)	150(2)	150(2)	150(2)
reflns collect.	100204	123551	93781
unique reflns	16765	16626	16783
R_{int}	0.0385	0.1374	0.0587
R1 [$I>2\sigma(I)$]	0.0718	0.0810	0.0718
*w*R2 (all data)	0.1053	0.1808	0.1380
CCDC No.	2377595	2377596	2377597

3. Computational methods and details

Computational experiments were performed using the Gaussian 16 program.[8] Geometry optimization was carried out at the B3LYP level with the def2-TZVP basis set for the transition metal (*i.e.*Fe, Co, Ni), and the def2-SVP basis set for all other atoms.[9] In all cases, the reduced ligand structure IXyl was used in place of IPr (IXyl = [(H)CN(Xyl)C:]; Xyl = 2,6-Me_2-C_6H_3; IPr = [(H)CN(Dip)C:]; Dip = 2,6-^{i}Pr$_2$-C_6H_3), and the methyl group of toluene was removed. Stationary points were confirmed as true minima by vibrational frequency analysis (no negative eigenvalues). For Fe, a spin state of 3/2 was calculated, for Co a spin state of 1 was calculated, and for Ni a spin state of 1/2 was calculated. Calculated structures were visualised using the ChemCraft program.[10]

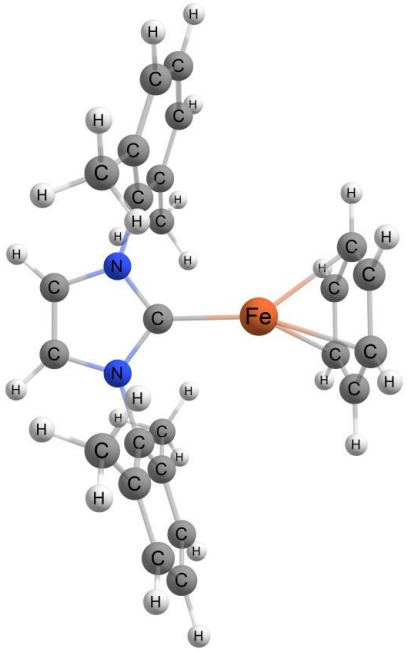

Figure S44. The calculated lowest energy conformation for the S = 3/2 spin-state of [IXyl·Fe(η_6-benz)]$^+$.

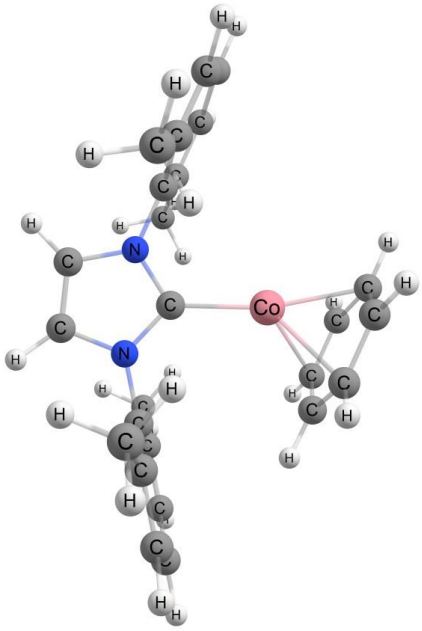

Figure S45. The calculated lowest energy conformation for the S = 1 spin-state of [IXyl·Co(η_6-benz)]$^+$.

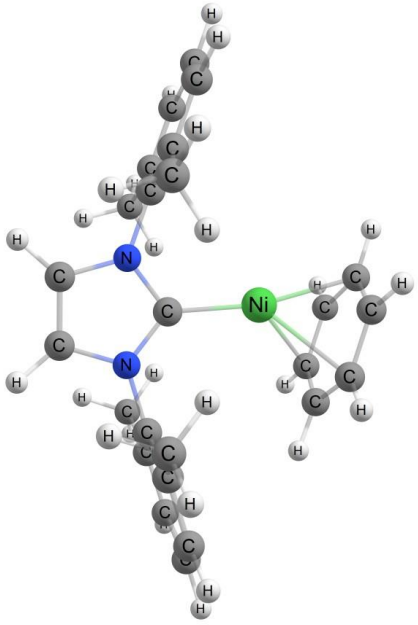

Figure S46. The calculated lowest energy conformation for the S = 1/2 spin-state of [IXyl·Ni(η_6-benz)]$^+$.

Table S3. Cartesian geometry of [IXyl·Fe(η_6-benz)]$^+$.

Atom	x-coordinate	y-coordinate	z-coordinate
Fe	0.00034	1.22825	-0.49186
N	1.08028	-1.54764	0.19707
N	-1.07622	-1.54903	0.19702
C	-2.45135	-1.11613	0.10545
C	0.00153	-0.73052	0.03409
C	2.45483	-1.11284	0.10551
C	3.11098	-0.70015	1.28269
C	-3.0864	-1.14249	-1.15261
C	2.41381	-0.71203	2.62079
C	-0.67756	-2.8529	0.46262
H	-1.39179	-3.65551	0.62521
C	-3.10832	-0.70519	1.28279
C	3.09013	-1.13914	-1.15242
C	0.68332	-2.85201	0.46269
H	1.3986	-3.65366	0.62542
C	4.4454	-0.28437	1.16935
H	4.98043	0.0381	2.06599
C	4.42539	-0.71377	-1.2131
H	4.94451	-0.72637	-2.17452
C	-2.41133	-0.71693	2.62098
C	-4.42224	-0.71891	-1.21325
H	-4.94116	-0.73162	-2.17478
C	2.37491	-1.61854	-2.39223
C	-2.37039	-1.62029	-2.39258
C	-4.44329	-0.29117	1.16949
H	-4.97894	0.02991	2.06625
C	-5.09362	-0.29568	-0.06555
H	-6.13599	0.02485	-0.13249

C	5.09597	-0.28884	-0.06555
H	6.13791	0.03309	-0.13251
C	0.696	2.99958	1.16102
H	1.23747	2.91084	2.10464
C	1.40303	3.14431	-0.04127
C	0.71093	3.20539	-1.27037
H	1.26246	3.3171	-2.20587
C	-0.71901	2.99614	1.15453
H	-1.26871	2.90426	2.09306
C	-1.41573	3.13775	-0.05417
H	-2.50789	3.1491	-0.0554
C	-0.71276	3.20225	-1.27686
H	-1.25622	3.31145	-2.21736
H	1.49035	-1.00151	-2.6218
H	2.01777	-2.6553	-2.28222
H	3.04143	-1.58569	-3.2646
H	-2.01237	-2.65683	-2.2832
H	-1.48632	-1.00233	-2.62147
H	-3.03671	-1.58743	-3.26511
H	2.49509	3.16082	-0.03263
H	-1.4955	-0.1039	2.60825
H	-2.10744	-1.73537	2.91351
H	-3.07126	-0.3291	3.40899
H	1.497	-0.1005	2.60749
H	3.073	-0.32256	3.4086
H	2.11157	-1.73078	2.914

Table S4. Cartesian geometry of [IXyl·Co(η_6-benz)]$^+$.

Atom	**x-coordinate**	**y-coordinate**	**z-coordinate**
Co	-0.18931	1.32569	-0.00055
N	-1.22768	-1.48036	0.00094
N	0.92568	-1.56126	0.00094
C	-0.11921	-0.68766	0.00054
C	-2.58136	-0.97303	0.00072
C	2.97542	-1.02601	1.23758
C	0.47627	-2.87448	0.00158
C	2.3213	-1.189	0.00069
C	-0.88469	-2.82378	0.00159
C	-3.21667	-0.74666	-1.23754
C	-2.52582	-1.0356	-2.54813
C	-3.21577	-0.74316	1.23884
C	2.97552	-1.02799	-1.23639
C	-4.52906	-0.2532	-1.21018
H	-5.04782	-0.06923	-2.15407
C	4.3308	-0.66512	1.21105
H	4.8656	-0.5346	2.15501
C	4.3309	-0.66705	-1.21032
H	4.86576	-0.53799	-2.15445
C	-2.52374	-1.02795	2.54971

C	-4.52817	-0.24984	1.21104
H	-5.0463	-0.06328	2.15477
C	2.25551	-1.23509	2.54723
C	2.25575	-1.23919	-2.54579
C	-5.17765	-0.00546	0.00031
H	-6.20183	0.37492	0.00017
C	1.22868	2.63701	-1.22491
H	1.72602	2.41431	-2.17031
C	5.00176	-0.48429	0.00024
H	6.05917	-0.20925	0.00007
C	-0.08003	3.17204	-1.22434
C	-0.73253	3.45283	-0.00076
H	-1.74299	3.86524	0.00032
C	1.88308	2.37299	-0.00353
H	2.88152	1.93261	-0.00455
C	-0.0771	3.17289	1.22144
H	-0.58638	3.36638	2.16762
C	1.23158	2.63785	1.21924
H	1.7312	2.41582	2.16359
H	-1.62977	-3.61474	0.00199
H	1.15949	-3.71953	0.00201
H	-0.5916	3.36476	-2.16943
H	1.39071	-0.56396	-2.64881
H	1.86932	-2.26735	-2.63749
H	2.92909	-1.06086	-3.39521
H	-1.58612	-0.46903	-2.65206
H	-3.17315	-0.77366	-3.39592
H	-2.26577	-2.10247	-2.6445
H	1.86811	-2.26278	2.64011
H	1.39111	-0.55892	2.64951
H	2.92903	-1.05641	3.39643
H	-2.25836	-2.0934	2.64689
H	-3.17242	-0.76846	3.39723
H	-1.58688	-0.45656	2.65338

Table S5. Cartesian geometry of [IXyl·Ni(η_6-benz)]$^+$.

Atom	**x-coordinate**	**y-coordinate**	**z-coordinate**
Ni	0.19043	1.24025	0.00021
N	-0.91136	-1.58089	-0.00028
N	1.24262	-1.4851	-0.00026
C	0.12849	-0.70232	-0.00021
C	-2.30661	-1.21068	-0.00024
C	3.22073	-0.72318	-1.23814
C	-2.96138	-1.04761	1.23662
C	2.5886	-0.96106	-0.00015
C	0.90731	-2.83317	-0.00042
H	1.65855	-3.6182	-0.00049
C	-0.45158	-2.89398	-0.00043
H	-1.1293	-3.74327	-0.00058

C	-4.31666	-0.68614	1.21056
H	-4.85164	-0.55698	2.15464
C	-2.96117	-1.04656	-1.23705
C	3.22066	-0.72353	1.23796
C	4.526	-0.21123	-1.21065
H	5.04199	-0.01899	-2.15446
C	-4.31646	-0.68512	-1.21091
H	-4.85129	-0.55518	-2.15498
C	2.53302	-1.02065	-2.54833
C	4.52592	-0.21156	1.2107
H	5.04186	-0.01956	2.15458
C	2.53283	-1.02131	2.54802
C	-4.98753	-0.50394	-0.00016
H	-6.04514	-0.22953	-0.00013
C	5.17148	0.04383	0.00007
H	6.19034	0.43831	0.00017
C	-1.92457	2.4226	0.00236
H	-2.932	2.00193	0.00374
C	-1.28008	2.68865	-1.22236
C	0.03523	3.19022	-1.22666
H	0.54503	3.39489	-2.17008
C	-1.2769	2.6892	1.22525
H	-1.79093	2.49559	2.16842
C	0.69878	3.42655	-0.00135
H	1.72283	3.8054	-0.00276
C	0.03848	3.19069	1.2258
H	0.55081	3.39572	2.16778
H	-1.79661	2.49453	-2.16405
C	-2.24035	-1.25482	-2.54634
C	-2.24079	-1.25709	2.54584
H	-1.38128	-0.57502	2.65124
H	-1.84521	-2.28196	2.63399
H	-2.91595	-1.08697	3.39554
H	1.58524	-0.46772	2.64904
H	3.17551	-0.74997	3.39648
H	2.2876	-2.09168	2.64423
H	1.58528	-0.46729	-2.64917
H	2.28809	-2.09106	-2.64494
H	3.17565	-0.74883	-3.39666
H	-1.38178	-0.57152	-2.65162
H	-2.91576	-1.08539	-3.39598
H	-1.84335	-2.27911	-2.63473

4. References

[1] A. R. O'Connor, C. Nataro, J. A. Golen, A. L. Rheingold, *Journal of Organometallic Chemistry* **2004**, *689*, 2411-2414.

[2] J. Cheng, J. Liu, X. Leng, T. Lohmiller, A. Schnegg, E. Bill, S. Ye, L. Deng, *Inorganic Chemistry* **2019**, *58*, 7634-7644.

[3] J. Du, L. Wang, M. Xie, L. Deng, *Angewandte Chemie International Edition* **2015**, *54*, 12640-12644.

[4] M. R. Elsby, S. A. Johnson, *Journal of the American Chemical Society* **2017**, *139*, 9401-9407.

[5] M. Muhr, P. Heiß, M. Schütz, R. Bühler, C. Gemel, M. H. Linden, H. B. Linden, R. A. Fischer, *Dalton Transactions* **2021**, *50*, 9031-9036.

[6] G. M. Sheldrick, SHELXL-97, Program for Crystal Strucutre Refinement, Göttingen, 1997.

[7] G. Sheldrick, *Acta Crystallogr., Sect. C: Struct. Chem.*, **2015**, *71*, 3-8.

[8] M. J. Frisch, G. W. Trucks, H. B. Schlegel, G. E. Scuseria, M. A. Robb, J. R. Cheeseman, G. Scalmani, V. Barone, G. A. Petersson, H. Nakatsuji, X. Li, M. Caricato, A. V. Marenich, J. Bloino, B. G. Janesko, R. Gomperts, B. Mennucci, H. P. Hratchian, J. V. Ortiz, A. F. Izmaylov, J. L. Sonnenberg, Williams, F. Ding, F. Lipparini, F. Egidi, J. Goings, B. Peng, A. Petrone, T. Henderson, D. Ranasinghe, V. G. Zakrzewski, J. Gao, N. Rega, G. Zheng, W. Liang, M. Hada, M. Ehara, K. Toyota, R. Fukuda, J. Hasegawa, M. Ishida, T. Nakajima, Y. Honda, O. Kitao, H. Nakai, T. Vreven, K. Throssell, J. A. Montgomery Jr., J. E. Peralta, F. Ogliaro, M. J. Bearpark, J. J. Heyd, E. N. Brothers, K. N. Kudin, V. N. Staroverov, T. A. Keith, R. Kobayashi, J. Normand, K. Raghavachari, A. P. Rendell, J. C. Burant, S. S. Iyengar, J. Tomasi, M. Cossi, J. M. Millam, M. Klene, C. Adamo, R. Cammi, J. W. Ochterski, R. L. Martin, K. Morokuma, O. Farkas, J. B. Foresman, D. J. Fox, **2016**.

[9] (a) A. D. Becke, *J. Chem. Phys.* **1997**, *107*, 8554–8560; (b) F. Weigend, R. Ahlrichs, *Phys. Chem. Chem. Phys.* **2005**, *7*, 3297; (c) J.-D. Chai, M. Head-Gordon, *J. Chem. Phys.* **2008**, *128*, 084106; (d) S. Grimme, J. Antony, S. Ehrlich, H. Krieg, *J. Chem. Phys.* **2010**, *132*, 154104.

[10] Chemcraft - graphical software for visualization of quantum chemistry computations. Version 1.8, build 682. https://www.chemcraftprog.com.